# WALL CONFINEMENT EFFECT IN PARALLEL FLOW INDUCED VIBRATION
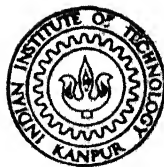
By

SHAH NAWAZ MOHD. MALIK

DEPARTMENT OF MECHANICAL ENGINEERING
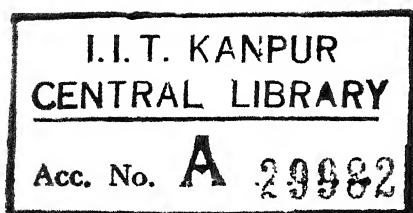INDIAN INSTITUTE OF TECHNOLOGY KANPUR
JULY 1974

# WALL CONFINEMENT EFFECT IN PARALLEL FLOW INDUCED VIBRATION

A Thesis Submitted
In Partial Fulfilment of the Requirements
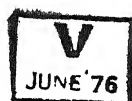for the Degree of
MASTER OF TECHNOLOGY

By
SHAH NAWAZ MOHD. MALIK

to the

DEPARTMENT OF MECHANICAL ENGINEERING
INDIAN INSTITUTE OF TECHNOLOGY KANPUR
JULY 1974

# CERTIFICATE

This is to certify that the thesis entitled "Wall Confinement Effect in Parallel Flow Induced Vibration" by Shah Nawaz Mohd. Malik is a record of work carried out under my supervision and has not been submitted elsewhere for a degree.

24th July 1974

V. Sundararajan
Associate Professor
Department of Mechanical Engineering
Indian Institute of Technology Kanpu

## ACKNOWLEDGEMENT

# CONTENTS

# LIST OF FIGURES

# LIST OF PLATES

## NOMENCLATURE

$\emptyset$      : Test Rod diameter (outer) in Inches.

t      : Wall thickness of the Test Rod in Inches.

$\psi$      : External Flow Tube diameter in Inches.

$\zeta_W$      : Damping factor with partially filled Flow-Tube.

$\zeta_{NW}$      : Damping factor with no water in the Flow-Tube.

$\zeta_F$      : Damping factor at various flow velocities.

$\zeta_{NF}$      : Damping factor at no - flow and full water in the Flow-Tube.

$X_D$      : Vertical R.M.S. response (in Milli-Volts) of a test-rod in various Flow-Tubes.

$X_{LD}$      : Vertical R.M.S. response for the largest diameter Flow - Tube (here 2.5" $\psi$) at a velocity at which $X_D$ is measured.

d      : Diameter Ratio $\emptyset/\psi$ , a measure of wall confinement.

$\omega$      : Damped Natural frequency of the Test Rod in $H_Z$, measured from the damping plots.

Stiffness and mass ratio      : Ratio of stiffness or mass of the Test-Rod in question to the smallest size Test-Rod.

SYNOPSIS


of the
Dissertation on
Wall Confinement Effect in
Parallel Flow Induced Vibration

Submitted in Partial Fulfilment of
the Requirements for the Degree

of

MASTER OF TECHNOLOGY

in

MECHANICAL ENGINEERING

by

SHAH NAWAZ MOHD. MALIK

Department of Mechanical Engineering
Indian Institute of Technology Kanpur

JULY 1974

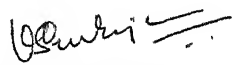An experimental investigation has been made to obtain the effect of wall confinement on the vibration of elastic cylinder held in parallel fluid flow. Four kinds of vibration parameter are studied in an open loop water tunnel with variable circular flow area (in steps): effect of partial water-level on the damping factor, effect of flow velocity on the damping factor, effect of flow velocity on the r.m.s. response and the effect on the power spectral density of response.

Experiments are carried out on aluminium tube with fixed-fixed end conditions. Four electrical resistance strain gages were fixed at half length to sense the signal in two perpendicular directions. Flow velocity was varied upto 60 feet/sec. Three different diameter test rods and external flow tubes were used.

Plots are given for different parameters as a function of flow velocity for each test rod in various external flow tubes. Comparison with available experimental results is made wherever possible.

The effect of wall confinement is to increase the various parameters studied here. But the rate of increase is more for the test rod with very low stiffness. However, if the two test rods have comparable stiffness the wall confinement has greater effect on the one with larger diameter (even if this test rod has greater stiffness).

# CHAPTER-I

## INTRODUCTION

### 1.1  General:

Analysis and prediction of dynamic behavior
of fluid coupled elastic system has a very wide range
of applications.  We can classify them broadly in three
categories:-

(1) Fluid-elastic instability of cylinders in cross-
flow.

(2) Stability of an elastic tube conveying flowing
fluid.

(3) Fluid coupled elastic stability of cylinders
in parallel flow.

All the three problems of dynamic interaction
have very important roles to play in the Nuclear Reactor
Core components design and performance, for example,
vibration of heat-exchanger tubes in cross-flow, bending
vibration of piping systems and the response of fuel rods
in parallel coolant flow to extract the heat generated
during the controlled nuclear fission process.  Both in
the Fast Breeder as well as in the Thermal reactors, high

velocity of the coolant is the primary source of energy
inducing the above mentioned instabilities.

Among the three, first one is the oldest problem
of hydrodynamic instability predicted by Th. Von Kármán;
while the second one was identified as early as in 1950
by Ashley and Haviland (1). But attention to the para-
llel flow induced vibration was given very recently during
the investigation of reactor core components failure.

In the nuclear reactor core, series of uranium
fuel pellets are contained in a metal cladding, forming a
fuel rod. Cladding material is a must for several rea-
sons, viz., retention of fission products, protection of
the fuel from the coolant, facilitation of insertion and
removal of fuel from the core and the exact location of
fuel within the core. Several of these fuel rods forming
a fuel cluster are fed into the coolant channel. The
axially flowing coolant induces transverse vibration of
fuel rods. Though the amplitude of vibrations are very
small but the close spacing of fuel rods create the prob-
lem of wear, fatigue and fretting.

It has been found that vibrating fuel rods may
also lead to incorrect flow distribution and the Neutron-
flux oscillations, resulting in random perturbations in

the reactivity and kinetic behavior of nuclear system (2).

In the present work, the flow induced vibrations of elastic cylinder in parallel flow will only be dealt with.

## 1.2 Previous Work:

First study of the parallel flow induced vibration was carried out by Burgreen, Byrnes and Beneforado (3) while studying the problem of heat transfer to the water flowing parallel to a bundle of rods simulating a water-cooled reactor core. Test were conducted on a vertical bundle of 13 and 37 rods in a closed flow loop. Data were collected for the mid point rod response and natural frequency at different flow velocities, using strain gage circuitory. Measurements revealed that the vibration occur at all the flow velocities and the amplitude increases with the velocity. Frequency of vibrations in water were lower than in still air and remained almost constant for a wide range of water flow velocity. These facts led to the conclusion that the oscillations were of self excited type rather than forced one (for example, due to Kármán vortices). Also, an analytical model was proposed using the force balance among flexural restoring force, damping and inertia force. Hydrodynamic force of water was identified as the forcing function. An emperical

relation for the response amplitude was given, using nondimensionalized parameters. Finally it was concluded that the parallel flowing fluid can excite oscillations at the natural frequency or more precisely at the damped natural frequency of the rods.

During the late '60s, number of flow induced vibration problems in reactor core components were observed notably in the reactors EBR II (4), GETR (5,1[*]), Big Rock-Point (6,2,3 and 4), Yankee (7, 5), SPERT III (8,1) and MSRE (9) etc.. These involved the problem of thermal power oscillations, fatigue, wear, mechanical failure of incore components and the neutron-flux oscillations. Though the occurance of such vibration problems were checked by redesign using trial and error but the mechanism of energy extraction and vibrational response propagation was not established clearly.

After Burgreen's work several experimental studies were conducted to predict the amplitude of vibration emparically in the United States (6 to 10), Sweden (11 to 13), France (14) and Canada (10, 11). In 1962, Quinn (7)

---

[*]  Digits with a bar represent the papers reported in bibliography.

Digits without bar represent the papers referred in the list of references.

performed tests on single and multiple rod assemblies
both in one and two phase flow. A mathematical model
was given and its solution was compared with the experi-
mental data. However, the mathematical model contained
several vaguely defined parameters and was difficult to
apply.

Paidoussis (10) collected the experimental data
of Quinn along with those of Swedish and French investi-
gators and tried to correlate with the Burgreen et.al.
emperical expression. He found deviations upto 10 times
for water tests and upto 100 times for super heated stream
tests. So, he himself derived the equation of motion for
the transverse vibration of a beam in axial flow using
the force balance technique involving the following
forces :

    (1) flexural rigidity of the beam

    (2) longitudenal tension

    (3) force due to inertia

    (4) lateral fluid forces which are

        (i) reaction on the cylinder of the force

        required to accelarate the fluid around it (12),

     (ii) frictional normal drag force.

However, no account was given to the viscous and struc-
tural damping of the material.

Instead of solving the resulting equation of motion, Paidoussis gave an emperical relation for the mid rod displacement in terms of non-dimensionalized parameters of the equation of motion. Exponent of each parameter was found by keeping the other parameters fixed and plotting the vibration amplitude with respect to the parameter in question. He admitted that a better correlation can be obtained using the variables involving cross-flow, swirl velocity and surface roughness which were neglected owing to the absence of experimental data.

Further work of Paidoussis (11, 13, 14) deals with the solution of the governing equation of motion in the form of $Y(\xi) e^{i\omega t}$, where $\omega$ is the dimensionless complex frequency. The solution for the complex frequency $\omega$, for the given system parameters, as a function of non-dimensionalized flow velocity was plotted on the Argand Diagram. It was predicted that system will be stable when the imaginary component of $\omega$, $I_m(\omega) > 0$ and unstable when $I_m(\omega) < 0$, $I_m(\omega) = 0$ gave the condition of neutral stability.

The stability in the three lowest mode was considered. The stability diagrams indicated that the motion of cylinder will be damped out at lower flow

velocities (Real component of $\omega$ , $R_e(\omega)$ decreases) and at higher flow velocities system becomes unstable. However the first mode instability was of buckling type ($I_m(\omega) = R_e(\omega) = 0$) and the higher mode instabilities were oscillatory ($R_e(\omega) \neq 0$). These trends were almost similar for all types of boundary conditions viz. pinned, clamped and clamped-free.

The presence of these instabilities were also established experimentally using cast rubber cylinders in a water flow-loop. Critical flow velocities for buckling and higher modes were measured and found to be close to the predicted analytical values. However, these hydro-elastic instabilities occured at very high flow velocities not to be encountered in the present day reactor technology. These "sub-critical vibration" were postulated to be due to the cross-flow component of axial flow velocity produced owing to non-uniform flow passages, secondary circulation, turbulence and separation behind the structures supporting the cylinder. It was anticipated that even in the smooth flow conditions (with White Noise spectrum) cylinder will extract energy from the noise spectrum corresponding to its normal mode and will be set into motion.

In his later work (15), Paidoussis modified the emperical relation predicting the mid rod displacement

on the basis of experiments on single cylinder with
different mass, length, flexural rigidity, diameter,
different flow conditions and method of supporting the
cylinder. It was found that the swirling motion will
increase the amplitude by a factor of 10 to 100 times
above the predictions. Experiments with a bundle of 19
cylinders indicated the increase in vibration amplitude
by a factor of 50 to 100, even in the quite flow conditions.
However, at higher flow velocities this factor gradually
reduced to a value of 5 to 10 with respect to the emperical
predictions.

Analytical work carried out by Burgreen et.al (3)
Quinn (7) and Paidoussis (10) etc. identifies the visco-
sity of flow medium as the major factor affecting the
vibration, whereas the experimental results do not conform
it precisely. Y.N. Chen (32) postulated the turbulence
in the flow as the major factor exciting the vibration.
He considers the vibration to be the self excited one
because the turbulence in the flow will cause rod osci-
llations which in turn will further increase the turbu-
lence in the boundary layer. He formulated the dynamical
equation involving the longitudinal surface drag force,
inertia force of the rod, normal drag of the lateral flow
and the centrifugal force of the flow on the rod (due to

its curvature). Inertia force due to Coriolis accelera-
tion was neglected on the assumption of smaller angular
velocity having mixed derivative term ($\frac{\partial^2 y}{\partial x \, \partial t}$). Axial
flow velocity was assumed to be the sum of mean flow velo-
city and a fluctuating component due to the turbulence.
Governing equation of motion of the system was then sim-
plified to the Mathieus type differential equation. Sta-
bility criteria was established on the basis of critical
flow velocity that results in the buckling of the rod. .
As the turbulence in the flow has a broad frequency spec-
trum, so a degree of instability of the rod will always
be excited. But the instability may be easily excited if
the strength of turbulence is high at a frequency near
the rod natural frequency.

Experimental data of Burgreen (3), Quinn (7),
Sogreah (14), Pavlica and Marshall (10), Roström (11) were
used to find the functional dependence of non-dimensiona-
lized vibration amplitude on the flow velocity. Exponent
found in this manner agreed very well with the Chen's
theoretical predictions. Finally it was concluded that
the rod vibration will not grow to a great extent because
of the unsteadiness in the phase of flow velocity
fluctuations.

During the late '60s, much progress in the flow induced vibration field was achieved. The concept of probabilistic and random nature of pressure field was first introduced by Reavis (16) and was used later by Gorman (17, 18), Chen and Wambsganss (21, 22, 23). Reavis analysed the first mode response of a pin-ended beam subjected to random pressure. Major assumptions were,

(1) pressure field of turbulent air flow in a duct was assumed to be identical to that of water flowing over a cylinder

(2) beam supports were assumed to be motionless and have no effect on the homogeneous pressure field. Comparison of theoretical values of the response with experimental results of Burgreen (3), Quinn (7), Pavlica and Marshall (8) and SOGREAH (14) indicated the experimental data to be higher by a factor ranging from 3.5 to 420, with 14 a representative value. He finally attempted to find the average disparity ratio between theoretical and experimental results and concluded that the lateral and longitudinal correlation density of random pressure field should be modified.

Using the results of Reavis (16) and wall pressure correlation data of Bakewell (19); Gorman (17) gave modified analytical expressions for the longitudinal and

peripherial spatial correlation densities on the basis of
his own experimental measurements. Damping coefficient of
the rod was determined at various flow velocities. Com-
parison of experimental and analytical predictions of
r.m.s. displacement (in a vertical plane) indicated good
agreement (maximum difference of 20% was found). This led
to the justification that the vibrations are predominantly
due to pressure fluctuations in the turbulent boundary
layer around the rod. Motion of the rod and supports was
also identified as a source of input energy. However, the
leading draw-back of his measurements was the assumption
of the same boundary layer properties at the surface of
test element and at the external flow tube wall.

Further work of Gorman (18) deals with the vibra-
tion of cylinder in two phase flow using air and water
mixture. In two phase flow, pressure fluctuations were
attributed to the change in lateral momentum flux of the
fluid as these are reflected from the fuel rod, unlike the
one phase flow where it was due to the lateral movement
of eddies. Measurements were taken for longitudinal and
prepherial correlation coefficients, damping plots and
r.m.s. rod response at various flow velocities and quality
of air-water mixture. With the increase in simulated steam
quality, displacement increased and a peak was obtained

at 12% steam quality followed by a gradual decrease in response amplitude. Longitudinal correlation coefficient increased rapidly with the steam quality to reach a first peak, it falls of f some what and then further increased with the steam quality. However, the peripherical correlation remained almost constant with the increase in steam quality. The damping coefficients were found to be about 4 times higher than those for one phase flow and exhibited the linear damping law, but the damping was almost independent of the steam quality.

Gorman's next attempt (20) was on a bundle of seven rods in two phase flow. Central rod was instrumented while the other six rods were used to simulate the actual flow and formations of sub-channels. Analytical model was further simplified, by using the result of his earlier work (18), to express the r.m.s. response explicitly as a function of power spectrum of the pressure drop corresponding to the rod fundamental frequency. Both the energy input as well as the response in a bundle was found higher than a single rod. Experimental data also revealed that for different mass flow rate, vibration amplitude attained a peak value at 16% quality and then either fell-off or held constant. Motion of the central rod in a bundle was purely

random and did not exhibit any preferred plane of oscilla-
tion. Though it was assumed that the random pressure
field around the central rod in a bundle is homogeneous,
but no justification was given for the basis of thinking
so.

The first rigorous treatment of the problem was
given by Chen and Wambsganss (21) using the Reavis (16)
approach on the equation of motion given by Paidoussis (13).
The statistics of boundary layer pressure field was based
on Bakewell's (19) measurement on a body of revolution.
Vibrations were postulated to be induced mainly due to
near field turbulent boundary layer pressure fluctuation.
Terms for damping (associated with the Internal visco-
elastic effect and external viscous effect) and random
pressure were included in the governing equation of motion*
for the rod with simply supported end condition. Due to
presence of mixed derivative Coriolis force term, $\dfrac{\partial^2 y}{\partial x\, \partial t}$,
the system does not possess classical normal modes. The
equation of motion was simplified by neglecting the
Coriolis force, damping and variable coefficient terms
to obtain a set of orthogonal eigenfunction as the solu-
tion of resulting equation which was coupled in nature.
Decoupling was established by neglecting the off diagonal
terms resulting in a set of equations representing the

---

* Please see Appendix-1.

normal modes of beam vibration. Power spectrum of the
rod response was found with the help of system response
function, spectral density of boundary layer pressure
field and the joint acceptance (representing the effec -
tiveness of the pressure in exciting a particular mode of
the rod vibration).

Expressions for the statistics of turbulent wall
pressure spectrum were found out, based on the analytical
model of Corocos (24) and experimental data of Bakewell (19),
Clinch (25) and Willmarth and Wooldridge (26). It is
worthwhile to note that Willmarth and Wooldridge found
the large energy density of the boundary layer pressure
at low frequencies. Parameter study to find the influence
of each parameter on the rod response was conducted for
the range encountered in the present day reactor techno-
logy. It was suggested that the r.m.s. response is pro-
portional to the flow velocity with a power of 1.5 to 2.0.
Comparison of the exponents of various parameters with
that of Burgreen et. al. (3), Paidoussis (15) exhibited
close similarities.

In the later work, Chen and Wambsganss (23)
modified the earlier analytical model to accommodate any

type of boundary condition and gave expression for the
effect of adjacent rod or proximity to the wall on the
virtual added-mass of the rod. Using the force balance
method they derived the equation of motion. However the
exact solution was difficult to be found out owing to
three reasons:

    (1) problem is non-self adjoint type

    (2) system does not possess classical normal modes

    (3) equation of motion contained variable coefficient
        term.

The resulting equations, after neglecting the Coriolis
force term ($\frac{\partial^2 y}{\partial x\, \partial t}$), damping, variable coefficient and
the terms associated with $\partial y / \partial x$ , were used to find an
adjoint system of equations such that these have same eigen-
values and the two set of eigenfunctions are biorthogonal.
Modal expansion technique with Galerkin's method was used
on the governing equation of motion in conjunction with
the set of biorthogonal eigenfunction to obtain a set of
ordinary differential equations. Decoupling of the system
of equations was obtained by neglecting the off-diagonal
terms on the basis of their smaller values. Solution for
r.m.s. displacement was obtained in terms of system res-
ponse function, power spectrum of random pressure and the
longitudinal cross correlation of random pressure.

Expressions for power spectral density of pressure field were modified on the basis of new experimental data of Wambsganss and Zaleski (22). Damping in a particular mode is the sum of three terms. viz.

(1) damping associated with internal viscoelastic and external viscous effects

(2) damping contribution of normal drag force

(3) damping due to Coriolis force.

The later two damping effects increase with the flow velocity. However, the damping contribution of Coriolis force depends on the end conditions. If the rod ends are not allowed to move (eigen value problem becomes self-adjoint), the Coriolis force ceases to give any contribution to damp the motion. If the rods are elastically supported or free at one end, the Coriolis force damping contribution becomes maximum surpassing the other damping effects.

Experimental investigations were carried out to find the dependence of fundamental frequency and damping coefficient on the flow velocity by applying external harmonic excitation using an electromagnet assembly. Comparison of experimental data with the analytical results indicated that for fixed-ends the frequency decreases with

the increase in flow velocity and the rod may be sub-
jected to buckling type instability at the critical velo-
city while for the cantilevered rods frequency increases
with the flow velocity and rod may be subject to flutter
type instability; both the damping and fundamental frequency
plots displayed a close agreement with the analytical
results.

Plots of r.m.s. rod displacement at the mid
point of fixed-fixed rod and at the free end of canti-
levered rod displayed a wide gap with respect to analy-
tical solution at low flow velocities (maximum difference
was as high as 300%). The lower values of prediction
were attributed to far field acoustic noise and structural
borne excitation which were not included in the analytical
model. Hydraulic diameter was also identified as an active
parameter. Lower hydraulic diameter means lower turbu-
lence level resulting in a smaller r.m.s. response. The
dependence of r.m.s. response of flow velocity was appro-
ximated by a power function relationship. The exponent
depends on damping, hydraulic diameter, flow noise and
rod support conditions.

However, no experimental attempt was made to find
the effect of adjacent rod or proximity to the wall on

the response, damping and natural frequency behavior.
Hence the effect of virtual mass on the response is yet
to be explored.

The latest work of Paidoussis (34, 16) also
takes into account the effect of gravity and external
pressure on the response of cylinder.  These two effects
are prominent if the cylinder is held in vertical confi-
guration and the system mean pressure is quite high.
Argand diagrams were modified to represent the stability
of the cylinder, when the above two effects are included.

## 1.3  Present Work:

. In the available literature no work (experimen-
tal, emperical or analytical) has been reported on the
effect of coolant flowtube wall on the response of
vibrating cylinders.  The present work has been initia-
ted with an aim to understand experimentally the adja-
cent wall effect on the flow induced vibrations of
flexible cylindrical rod in single phase (liquid) axial
flow.

Like the previous investigators, here also it
was assumed that the vibrations of elastic cylinder are
excited mainly due to random pressure fluctuations in

the turbulent boundary layer around the lateral surface of cylinder. Other possible sources of excitation are the motion of end supports and the pump flow pulsations etc.

Open loop water test-rig was designed, fabricated and installed to achieve water velocities well above the values encountered in the present day reactor technology. Test set-up has also the facility for varying the cross-sectional area of external flow tube (in steps) into which different diameter elastic cylinders are to be tested.

Strain gage circuitary has been used to find the mid rod response after proper amplification of the weak signals. Damping plots were recorded on the oscillograph both in full flow at different water velocities and partially filled flow tube with various water level (for example 1/2 filled, 3/4, 7/8 filled etc.). Owing to unknown distribution of forcing function (random pressure) it was difficult to convert the strain gage out-put into the displacement statistics; so, the strain values were used directly to represent the response of test rod. The rod end support conditions are fixed-fixed. Test data were also collected for the r.m.s. values of response signal using the random signal r.m.s.

voltmeter. Frequency response characteristics of the associated power spectrum was measured with the help of a band-pass filter by varying the central frequency of filtered input to the true r.m.s. voltmeter.

Finally the curves were plotted for the above mentioned parameters of damping factor, r.m.s. values of response and power-spectrum as a function of mean axial flow velocity for different diameter of external flow tube as well as the test rods. The effect of adjacent boundary wall of the flow tube on the response of the test rods was discussed from these graphs.

CHAPTER-II

EXPERIMENTAL SET-UP

## 2.1 General:

In this chapter details have been given for the test set-up, components fabricated and experimental procedure. The schematic diagram of the experimental set-up is presented in figure (1). Test set-up was designed to provide open-loop water circuit with variable flow velocity. Centrifugal pump used to supply the water has a capacity of 1000 gallons/minute at a head of 60 feet with 6 inch discharge pipe diameter. Since at high velocities major portion of head loss is due to friction losses in the pipe and the loss in 90 degree bends and elbows. So care has been taken to provide these in the low velocity regions, that is, in 6 inch diameter cross-sections. Because of lack of space in the pump room, the test section was installed on a separate flume and was connected to the pump by a 6 inch pipe line. To mak¬ the flow uniform, honey comb was fixed in the flow area at the upstream side. Diffusers with semi cone angle of 5 to 10 degrees were

used to reduce gradually the cross-sectional area from 6 inch to the desired test-section diameter*. To ensure further the flow to be uniform and fully developed, G.I. pipe of length greater than 40 diameters was connected to the upstream diffuser. This pipe length is connected to the perspex test section through flanges and bolts with rubber packing. Choice of perspex for the external flow tube was made owing to its high flexibility and ease in simulating actual conditions even at very low velocities. Aluminium tubes were selected as the test-rods due to their lower stiffness resulting in larger deflections. Test rod was supported axially into the external perspex flow tube through four mild steel pins at each end. At the downstream side of the test section a diffuser is again connected to increase the cross-section gradually to 6 inch diameter. Finally a 90 degree elbow is used to discharge the water vertically in the flume. Discharge from the flume was found by measuring the head over the V-notch. A time interval of about 5 minutes was needed to establish constant head over the V-notch for a particular gate valve opening. Mean-axial-flow velocity of water in the test section was calculated from the discharge values. Enough care was taken to make all the joints leak-proof.

---

* Please see the Appendix-2

## 2.2  Components Fabricated:

In the present work parts fabricated involved
mainly the following components:-

diffuser assembly, perspex external flow-tube
assembly, test rod supports and fixing pins,
flanges for 6 inch gate valve and pipe threading
on various diameter G.I. pipe line.

## 2.2.1  Diffuser Assembly:

To facilitate the change in cross-sectional area
of the external flow tube, diffusers were made out of 1/8
inch thick mild steel plate and were hot rolled manually
to conical shape.  One end was welded to 6 inch diameter,
1 foot length G.I. pipe and the other end to 6 inch length
of the desired flow-tube diameter G.I. pipe.  Finally the
flanges were mounted at the two threaded end of diffuser
assemblies.  To take out the strain gage lead wires, a
brass nipple was brazed to the smaller diameter side of
down-stream diffuser.

## 2.2.2  Perspex External Flow-Tube Assembly:

Flanges were made, using perspex sheet of 1 inch
thickness.  Flanges were bonded to the perspex tube with
the help of acetone.  Hub of the flange was also used to

fix the end supports of test rod using 4 mild steel fixing pins on its lateral surface. Details of a typical flange assembly for 2 inch diameter flow tube is given in the figure (2).

### 2.2.3 Test Rod Supports and Fixing Pins:

Aluminium test rod was supported at both the ends by means of test rod supports. These in turn were supported to the external perspex flow tube with the help of four 1/8 inch diameter mild steel fixing pins. Details of the test rod supports, made of mild steel, are given in the figure (3). It has three main parts: 1 inch length of diameter $d_1$ which press-fits in the internal diameter of aluminium test rod; section $d_1$ was joined to 1/2 inch diameter uniform section by the tapered portion; axial length of the uniform portion was kept 7/16 inch. Two 1/8 inch tapped holes at 180 degrees to each other were made along with a through hole of 1/8 inch diameter having 3/16 inch axial separation with respect to the tapped holes. Close dimensional accuracy was maintained to match these holes with those on the perspex flow tube mentioned in section 2.2.2. Finally the upstream and down-stream end was made stream lined to avoid flow separation. In the down stream rod support, central hole was drilled

and connected to a drilled hole on its lateral surface to take out the strain gage lead wires coming through the annulus of the test rod.

To support the test rod structure in the external flow tube, two 1/8 inch fully threaded pins were screwed in the tapped holes of the rod support and a long mild steel pin threaded at one end was passed into the through hole and screwed on the outer surface of perspex flow tube. In this way, fixing at 90 degree to each other in both the horizontal and vertical plane was achieved. The above mentioned precision work was carried out with close tolerances of the order of 0.005 inch.

2.3 Test Rod and Flow Tube Dimension:

In the present study of the adjacent flow tube wall effect on the response of test rods, following dimensions of the two were selected:

(1) Perspex flow tubes of internal diameter 2.5 inch, 2.0 and 1.0 inch with 1/8 inch wall thickness and 4 feet length.

(2) Aluminium hallow test rods of outer diameter 5/8 inch, 1/2 and 3/8 inch with the wall thickness of 0.049 inch, 0.0595 and 0.039 inch respectively and 46 inch length.

## 2.4  Experimental Procedure:

As outlined earlier, an elastic cylinder in axial flow will be set into oscillations, due to the random pressure distribution, in the turbulent boundary layer, upon its lateral surface.  Pressure distribution around the oscillating cylinder will be unsteady and non-stationary in nature because of departure from purely axial; uniform and steady flow.  The random forcing function on the test rod will result in the ramdomness of the response. Though the earlier investigators had identified the vibration to be of random in nature but they had attempted analytical solution as well as experimental measurements of response amplitude only in one particular plane, for example, vertical component.  Whereas in actual condition the amplitude of vibration will not be having any preferred plane of oscillation.  The actual response of the test rod can be found by measuring its component in two perpendicular planes.

There are several methods reported in earlier work for measuring the response of the test rod.  Paidoussis (15) used sub-miniature piezoelectric accelerometer screwed to the mid span of the rod and integrating the output twice to obtain the displacement signal.  Chen (23)

has used the optical displacement tracking technique.
Electrical resistance strain gages were used by Burgreen
et. al. (3) and Gorman (17). One other possible method,
now in use, is based on the principle of electro-magnetic
induction. Constant electro-magnetic field is applied
normal to the lateral surface of the test rod and a coil
is wound around the lateral surface of the rod where the
response is to be measured, so an e.m.f. will be induced
in a direction mutually perpendicular to the plane of
oscillations and plane of magnetic field. This e.m.f.
generated will depend on the number of turns in the coil
and the rate of magnetic flux linking the coil. The vol-
tage generated will represent the velocity of the test
rod in a direction perpendicular to the rod axes as well
as the magnetic field. However the system becomes very
expensive because a very large magnetic field is needed
to obtain measurable signal in a gap of 2 inch or more
between the magnetic pole pieces to accommodate the ex-
ternal flow tube in between it.

In the present work the resistance strain-gages
have been used because of their low cost, easier availa-
bility and good accuracy. To obtain actual response,
strain was measured both in horizontal and vertical plane.

To minimise the curvature effect, due to small diameter
of the test rod, gages of minimum possible dimension were
selected.

## 2.4.1. Test-Rod Preparation:

Bending strain at mid span was sensed using four
gages 90 degrees to each other. Gages were fixed on the
lateral surface of the test rod, parallel to the axes.
Lead wires were then passed into the annulus of the test
rod through the holes (1.5 m.m. diameter) on its lateral
surface. These holes were drilled on the down stream
side sufficiently far from the mid span to have negligible
effect on the response. Lead wires were finally taken out
of the downstream rod end support.

Water proofing of the strain gages is the crucial
part of the test rod preparation. Gages have to with-
stand following severe environmental conditions:-

(1) Leakage of water, humidity, moisture and thereby
absorbing water into the adhesive cement even at
no water flow conditions.

(2) Tangential viscous drag force on the test rod
which is a function of flow velocity.

A method of double protection, after some initial
gage failure, was finally used for water-proofing the gages.

A coat of melted cerese wax was applied over the gage
and the adjoining area upto lead wire and gage soldered
joint. Smoothness of the aluminium test rod surface in
the vicinity of gage installation was reduced using emery
paper and needle files to obtain proper bonding. The
liquid water proofing compound was then spread over the
entire area including the cerese waxed surface using hair
brush and acetone as thinner. Coating of the water proof-
ing compound was done twice with an interval of 24 hours.
Water proofing compound available in the domestic market
had a tendency to absorb atmospheric air in the form of
air bubles during its wet state. So, to avoid the possi-
bility of holes and vents, double coat of water, proofing
synthetic enamel paint was applied with 12 hours inter-
mediate drying time. Thickness of the total gage prepa-
ration was less than 1/8 inch.

## 2.4.2  Strain-Gage Circuit:

Both the strain gage pairs in horizontal and
vertical direction were connected separately to two bridge
balancing unit. Gages were connected to two adjacent
arms of each balancing unit in half bridge mode. This
will result in cancellation of signal due to temperature
and far field (acoustic) noise of the system. As outlined

by Wambsgnss (22), far field noise in the external flow, tube concentric with the test rod will give rise to the equal pressure contribution around the circumference of the test rod at a particular cross-section and at a particular instant. Hence, the response signal will be only due to near field flow noise of turbulent eddies. To amplify the output signal, both bridge balance units employed had a built-in amplifier of gain 50.

### 2.4.3. Damping Measurements:

Total system damping will be the contribution of several factors viz., structural damping of the test rod material, external viscous damping, damping due to normal drag force and Coriolis force. Damping due to these factors increases with the axial flow velocity except the structural damping. It is difficult to find the damping due to each factors separately. So, an attempt was made to find the equivalent viscous damping of the system. Initial deflection in horizontal gaged plane was given by attaching a weight to the steel wire (0.010 inch diameter) connected to the test rod. Diameter of the hole drilled in the perspex flow tube, through which the steel wire passes, was 0.012 inch to prevent any possible leakage. Damping plots at various flow velocities were

recorded on Visicorder Oscillograph by cutting the thread attached to the weight.  Sufficient care was taken to remove the noise components in the oscillograph, which is quite susceptible, due to the strong magnetic field of galvanometer assembly.

To find the effect of various water level on the damping behavior, plots were also taken for partially filled external flow tube.  Damping factor was calculated by measuring Logarithmic decreement in several successive cycles of damping trace.

## 2.4.4  R.M.S. Response Measurement:

R.M.S. value of the response, at various flow velocities, was measured by means of true r.m.s. voltmeter. Schematic circuit is given in Figure (4).  Output of the vertical and horizontal strain balancing units was fed to two D.C. amplifiers. of variable gain.  Output of each amplifier was then fed to the input of true r.m.s. meter. Gain of the D.C. amplifiers was adjusted to obtain measurable reading.  R.M.S. value of both the signals was read separately each at a time.  Because the random forcing function is unsteady in nature, so the r.m.s. meter pointer deflection was observed for 3 to 4 minutes and an average value was noted down.  Proper grounding of the equipments was done to minimise the noise in the electrical circuit.

## 2.4.5. Measurement of Response Spectrum Components:

Power spetral density of the response at different flow velocities was measured to find the major contribution at various frequencies. For this purpose a constant band pass, variable frequency, filter was used in series with the true r.m.s. voltmeter. Both the horizontal and vertical strain signals were fed, one at a time, to the filter and the centre frequency was varied continuously. Major r.m.s. components were read on the r.m.s. meter, after proper amplification of total signal to the variable filter. Here also an average reading of the meter was noted down to cope with the unsteady nature of the response signal.

Measurements outlined in section 2.4.3, 2.4.4 and 2.4.5 were taken for all the test rods using various size external perspex flow tubes.

## 2.5 Leading Specifications of the Instrument Used:

(A)    Visicorder Oscillograph

| | |
|---|---|
| Model | : 906T, Honeywell Inc. U.S.A. Ultraviolet light recording type. |
| Number of Channels: | Six (active) |
| Galvanometers | : M200-120, moving coil miniature type. |
| Frequency Response | : 0 to 120 Hz flat ($\pm$ 5%) |

| Current Sensitivity | : | 25.5 Micro-Ampere/inch. |
|---|---|---|
| Voltage Sensitivity | : | 1.58 Milli-Volts/inch. |
| Deflection | : | Traces may overlap, permitting a full 6 inch peak to peak amplitude. |
| Record Speeds | : | Four speeds selectable ranges 5, 25, 50 and 100 millimeters per second. |
| Recording Paper | : | Kodak Linagraph Direct Print type (using Latent Image Intensification process). |

(B)   Strain Indicator

| Model | : | Vishay/Ellis-10, Vishay Instruments Inc. U.S.A. |
|---|---|---|
| Function | : | Measurement of strain with half-bridge or quarter bridge strain gages. |
| Range of Resistance | : | 100 to 1000 ohms. |
| Resolution | : | ± 2 Micro-Strain. |
| Range | : | ± 5000 Micro-Strain. |
| Bridge Excitation | : | 4.5 Volt D.C. |
| SCOPE Output | : | (i) External load 100 Kohms or more:- <br><br> ± 0.5 Volt swing. <br><br> ± 5000 Micro-Strain, linear within 2%. <br><br> (ii) External load 200 ohms:- <br><br> ± 250 Micro-Ampere swing. <br> ± 1000 Micro-Strain, linear within 5%. |

(iii) Amplifier Characteristics:-

Single-ended output.

| | | |
|---|---|---|
| Frequency Response | : | Flat between 0 to 500 Hz. |
| Output Impedence | : | 500 ohms for a dynamic swing of $\pm$ 1000 Micro-Strain. |

## (C) Variable Filter

| | | |
|---|---|---|
| Model | : | 1-159-0001, Consolidated Electrodynamics Corpn. U.S. A. |
| Function | : | Constant percentage Band-Pass filtering with variable center frequency. |
| Bandwidth | : | 3% (constant) between 3 dB points. Minimum attenuation one Octave either side of the tuned frequency is 50 dB minimum. |
| Frequency Range | : | 8 to 2500 Hz (center frequency tuning range). |
| Input Impedance | : | 50 Kohms $\pm$ 2% |
| Noise Output | : | 1 Milli-Volts r.m.s. or less, with input shorted. |

## (D) R.M.S. Meter

| | | |
|---|---|---|
| Model | : | 55A06 Disa, Denmark. |
| Function | : | Root-mean-square voltage measurement of electrical signals irrespective of wave form. |
| Frequency Response | : | 3 Hz to 200,000 Hz. |
| Crest Factor | : | 5 : 1 |

| | | |
|---|---|---|
| Input Impedence | : | 1 Mega-ohm in parallel with 50 p.F. |
| Meter Response | : | Low or high damped. |
| Input Voltage Range | : | 0.2 Milli-Volt to 100 Volts. |
| Noise Level | : | Less than 50 Micro-Volt r.m.s. |
| Common Mode Rejection | : | 100 at 1000 Hz. |

(E)    Solid State Differential Amplifier

| | | |
|---|---|---|
| Model | : | TDA-875, Astrodata California (U.S.A.). |
| Function | : | Astrodata TDA series consists of amplifiers that are designed for use in missile checkout systems, in low-level instrumentation systems and in on-line control systems. They are for use in all cases in which high Common Mode Rejection, extraordinarily high input Impedence and high reliability are essential. |
| Voltage Gain | : | 1 to 2000 (11 fixed steps). |
| Mode of Operation | : | Single ended as well as Differential. |
| Input Impedence | : | Greater than 100 Mega-ohms in parallel with 0.0007 Micro-farad |
| Noise Level | : | Less than 5 Micro-Volts r.m.s. over the full frequency band. |

Single Ended Mode Operation :-

| | | |
|---|---|---|
| Grain Stability | : | DC to 1 Kc(within 0.1%). |
| Output Voltage | : | $\pm$ 10 Volts (maximum) from DC to 50 Kc. |

Load Resistance        :  Minimum 200 ohms.

Output Impedence       :  Less than 1.0 ohm in series
                          with 50 Micro-henries.

Frequency Response:       ± 1.0% , DC to 10 Kc.
                          Down 3 dB at 150 Kc.

Harmonic               :  Less than 0.1% r.m.s., upto
Distortion                10 Kc.

Differential Mode Operation :-

Frequency              :  ± 1.0% from DC to 300 Hz.
Response                  Down 3.0 dB at 5 Kc with
                          1000 ohms load.

Output Resistance      :  Less than 25 ohms

Load Resistance        :  Minimum 1000 ohms.

Output Voltage         :  ± 10 Volts (maximum) from
                          DC to 5 Kc.

Common-Mode            :  Greater than 120 dB at 60 Hz
Rejection                 for 1000 ohms of line
                          unbalance.

Common-Mode            :  300 Volts - step common mode
Level                     does not cause overload.

DC Gain                :  DC to 1 Kc (within ± 0.1%
Stability                 of the full scale)

(F)      Strain Gages

Model                  :  NKF-2, Rohits & Co., Roorkee,
                          India.

Gage Resistance        :  120 ohms (± 1.0%)

Gage Factor            :  2.68      (± 1.0%)

| | | |
|---|---|---|
| Strain Sensing Material | : | A Chromium-Copper alloy having traces of Si + Mn and it is recommended for dynamic strain measurements, because of its high temperature sensitivity and high gage factor. |
| Gage Dimensions | : | Grid length 2.0 millimeter<br>Grid width 0.5 millimeter<br>Base length 8.0 millimeter<br>Base width 5.0 millimeter<br>Hellical Grid. |
| Maximum Current | : | 40 Milli-Ampere. |
| Maximum Temperature Permissible | : | 80 degrees centigrade. |
| Cross-Sensitivity | : | 1.5% |
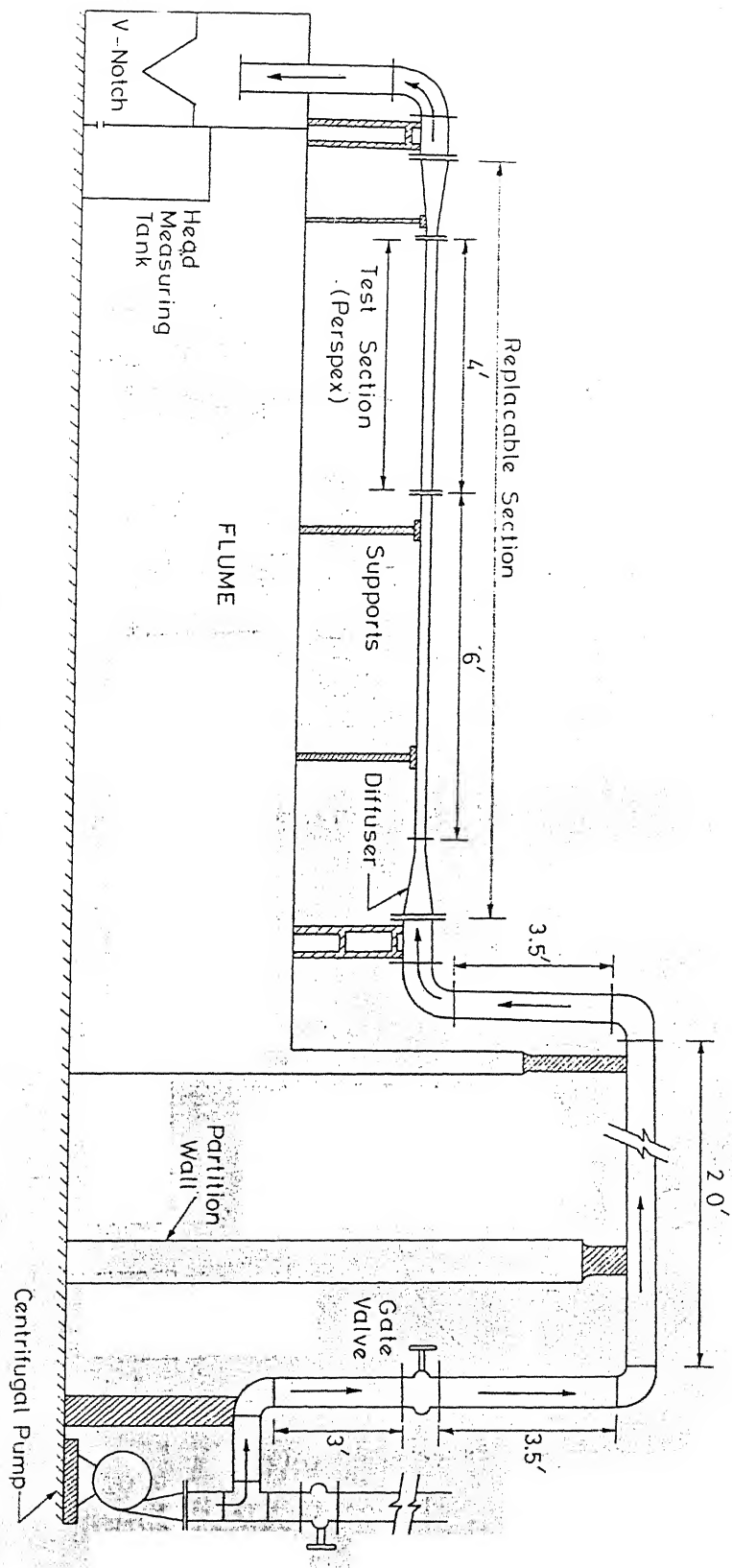
Test Set-up

FIG.-1

Flange Assembly Details



5.5  4.5  1/2  3/16  1/8  2  2.9  1/8 Drilled Hole  1/4  7/16

Loaded With Test-Rod



Test-Rod (1/2 inch)
Fixing Pin (1/8 inch)

5.5
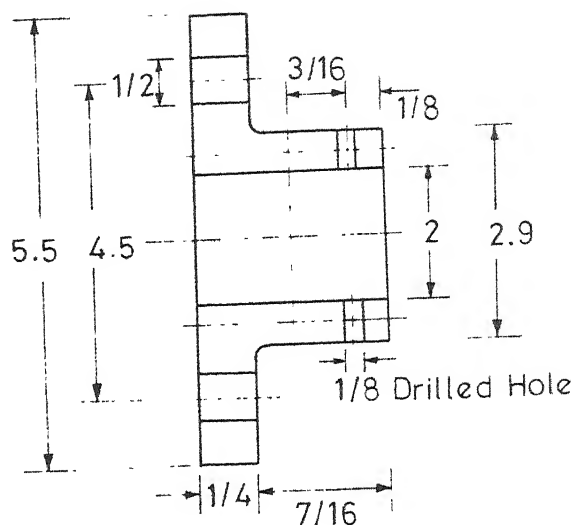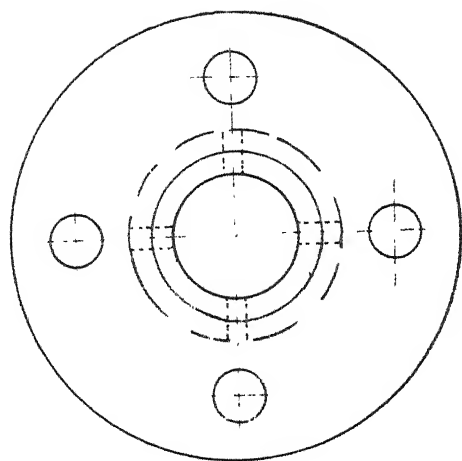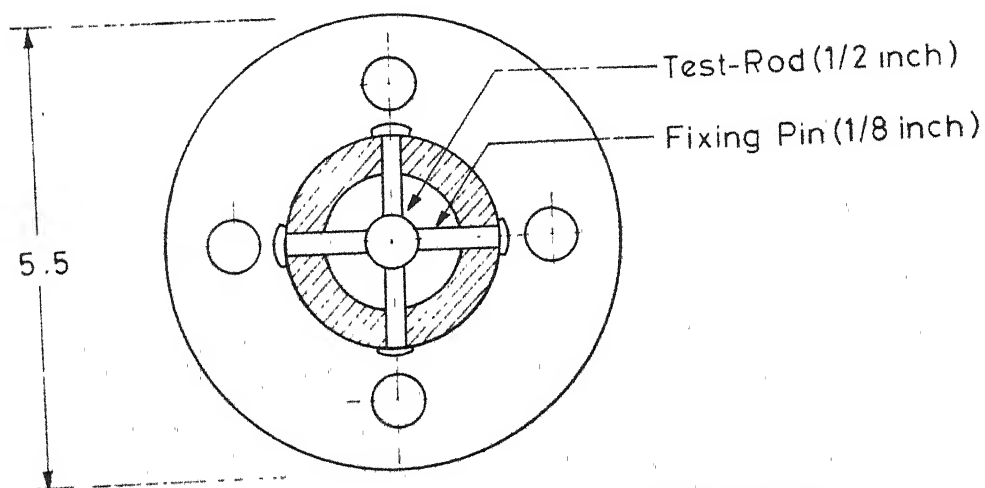
Material: Perspex
All Dimensions In Inches.

# Flange Assembly for 2inch Flow-tube

## FIG.-2

Upstream Support

7/16

1/2

$d_1$

1/8

1/8
Throug
Hole

1/2

Tapped Hole

1/8

1
9/16
1/8
3/16
1/8
1/4

Downstream Support

7/16

R

5/8

1/8

$d_2$ $d_1$

5/8

1/8
1/4
Hole

$(d_1 - d_2) = 1/8$

1/4
Drilled Hole

5/16
1/8
3/16
1/8
0/16
R
1
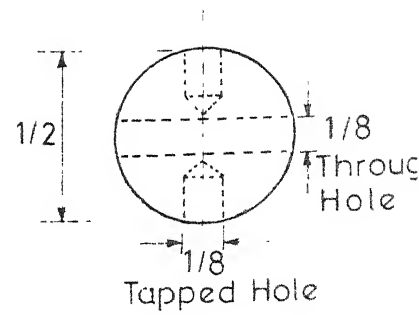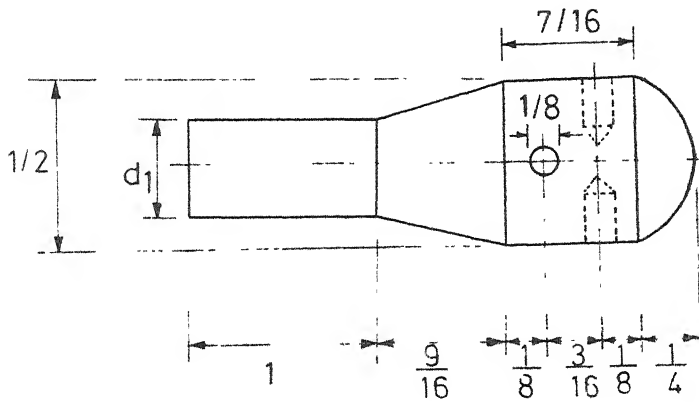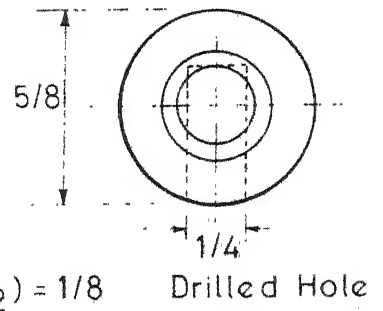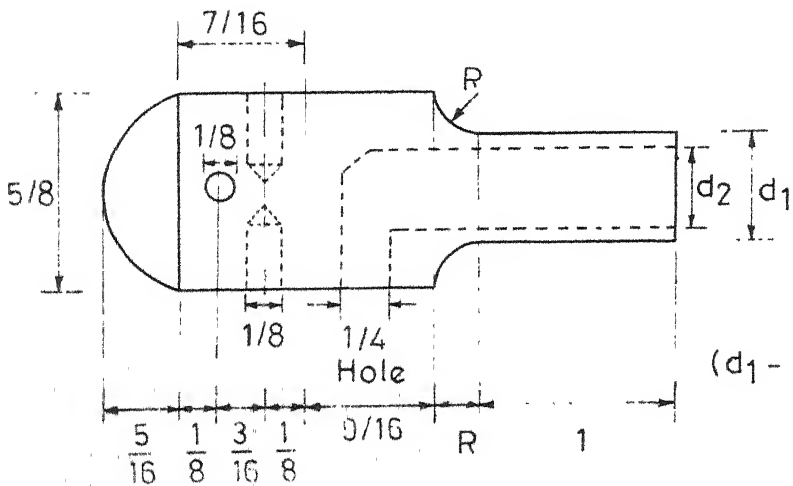
Material: Mild Steel
All Dimensions In Inches

# Test-Rod Supports

## FIG.-3
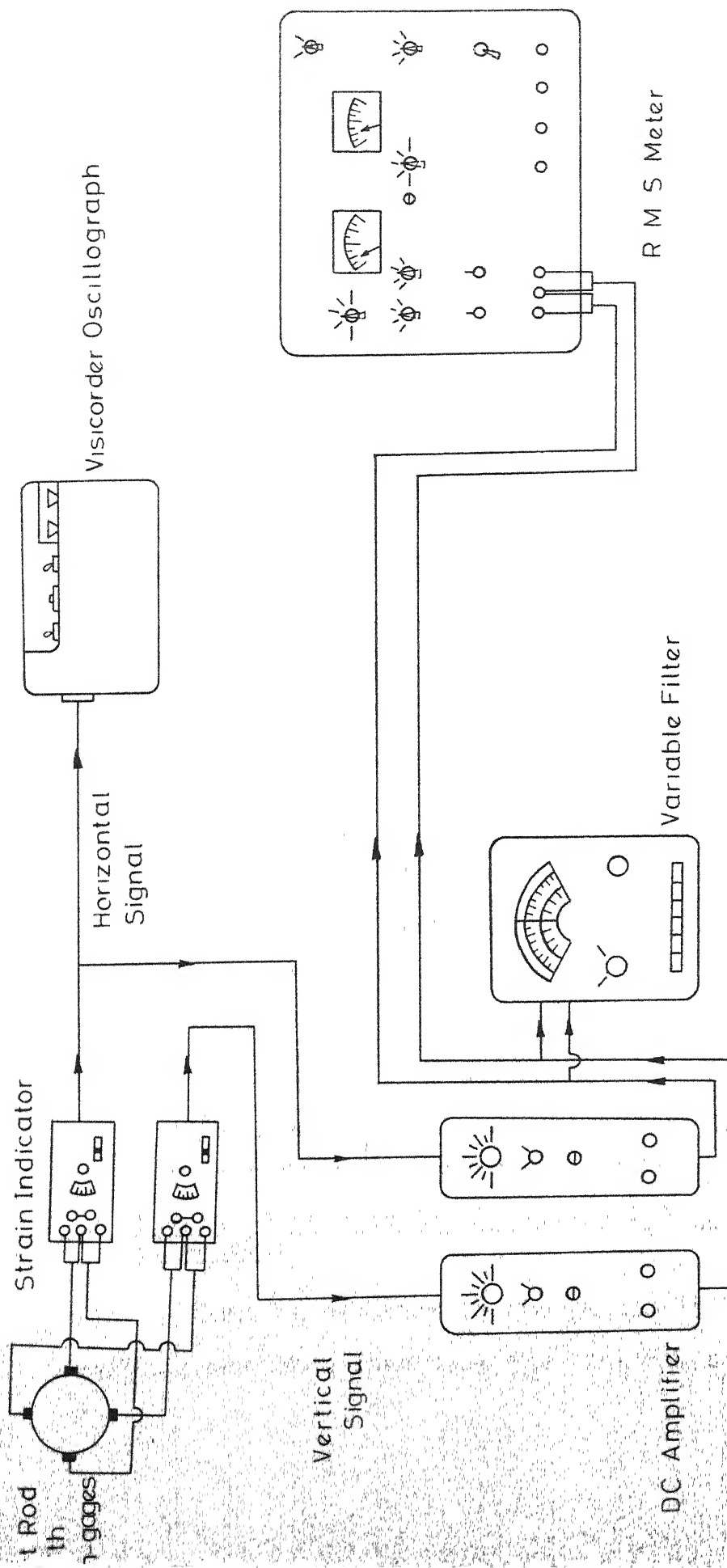
Electrical Circuit Diagram

FIG. - 4

CHAPTER-III

RESULTS AND DISCUSSIONS

## 3.1  General:

In this chapter, graphical plots and results have
been presented for the wall effect on the following parameters:

(1)  Damping factor in the partially filled external
flow tube.

(2)  Damping factor at various flow velocities.

(3)  R.M.S. response at various flow velocities.

(4)  Response power spectrum.

Theoretical stiffness and mass ratio for the
three test rods are tabulated below:

| Size | Stiffness Ratio | Mass Ratio |
|------|-----------------|------------|
| 3/8 inch | 1 | 1 |
| 1/2 inch | 3.95 | 2.085 |
| 5/8 inch | 6.6 | 2.18 |

## 3.2  Damping Factor in the Partially Filled External Flow-Tube:

Damping behavior in the partially filled tube is a
complex phenomenon involving the flexural structure subjected

to two fluids (having different density and viscosity) in a confined elastic conduit.

### 3.2.1 Graphical Plots:

Figs. 5,6,7 show the wall effect on the damping of test-rod at various water level in the flow tube. Increase in the damping factor, represented as $\zeta W/\zeta NW$, is taken as ordinate and the water level (0 to Fully-filled) as abscissa. Each figure was plotted for a particular size of test rod.

### 3.2.2 Discussion:

Damping values for no water, $\zeta NW$, for each rod with fixed  end conditions mounted in the different external flow-tube are fairly high (about 8 to 10 times the values of structural damping in a simple laboratory test.). This may be attributed to the end fixity conditions. Damping values $\zeta NW$ for a test rod in different flow tubes were also not same. This can be explained on the basis of the difference in rigidity of the rod supporting structure (which also include the perspex flow tube).

Fig. 5 shows the wall effect for the 3/8 inch diameter test rod. Damping increases with the water level. Even for 2.5 inch flow tube, there is a 55% increase in damping from zero to full water level. For 2.0 inch flow tube, water level above 3/4 has a faster rise in damping.

1.0 inch flow tube (area of cross-section being 1/6.25 of the 2.5 inch flow tube) gives the steepest rise in damping values upto 215%. We can infer that the wall effect is small for larger flow tubes filled upto 3/4th level and above this level it is considerable. For the smallest flow tube (wall confinement parameter d = 0.375) the damping factor is very sensitive when the tube is partially filled.

Fig. 6 shows the same trend, for a 1/2 inch test rod except that the rate of increase in damping is very low. For example, the increase in damping is 20% for 2.5 inch flow tube and 35% for 1.0 inch flow tube at full water level. Percentage increase in damping for the 1/2 inch test rod is quite less compared with the 3/8 inch test rod. This is due to larger stiffness of 1/2 inch test rod.

Fig. 7 shows the wall effect for the 5/8 inch test rod. Here the trends are slightly different. Maximum damping values are attained at approximately 1/2 water level and after that the damping remains constant upto full water level. However, the total percentage increase in damping is almost same as to that of 1/2 inch test rod (that is 25% for 2.5 inch flow tube and 38% for 1.0 inch flow tube). The change in behavior can be attributed to the damping due to normal drag force (which is a function of test rod surface area and, hence, dominant here) attaining its maximum value when the water level reaches 1/2.

Test rod damped natural frequencies are also tabulated in Figs. 5, 6 and 7. Natural frequencies are almost constant for each test rod and are quite independent of the water level in the flow tube. This shows that the confinement has very small effect on the natural frequency of vibration.

A comparison of all the three graphs show that the damping will increase at a faster rate and the wall effect will be prominent if the initial damping factor with no water is small.

### 3.3  Damping Factor at Various Flow Velocities

### 3.3.1  Graphical Plots:

Figs. 8,9 and 10 display the wall effect on the damping factor of the test rod at various flow velocities. The percentage increase in damping factor, $\delta F/\delta NF$, is plotted as ordinate for the same test rod, when mounted in the different flow tubes, with mean axial flow velocity as abscissa. Damping plots were taken for flow velocities upto 20 to 25 feet/sec; above which the damping plots became quite random in nature.

### 3.3.2  Discussion:

All the three figures show a linear increase in damping factor with flow velocity. This fact is identical

with the experimental results of Chen and Wambsganss(23) who
validated it theoretically also.

The damped natural frequencies of oscillation,
measured from the damping plots, remained almost constant at
various flow velocities as well as with wall confinement.
These have been tabulated in Figs. 5, 6 and 7. The effect of
flow velocity on natural frequency is identical in nature with
the previous results of Chen(23) and Burgreen et al(3). Chen
found a decrease in frequency of order of 4 to 5 % for a
velocity range of 0 to 100 ft/sec. From the values given in
Figs. 5,6 and 7  it can be inferred that the wall confinement
has negligible effect on the natural frequency at moderate
velocity range.

Fig. 8 shows the effect of wall on the damping factor
for a 3/8 inch test rod. Wall effect is quite prominent
even when the change is made from 2.5 inch to 2.0 inch extern⁑
al flow tube. For the 1.0 inch flow tube the percentage
increase in damping is large (for example 40% for a velocity
of 17 ft/sec). This trend is expected because the stiffness
of this test rod is very small and the normal drag force
increases with the flow velocity.

Fig. 9 gives the trend for 1/2 inch test rod.
Increase in damping with flow velocity and wall confinement

effect is small when the flow tube diameter is reduced from 2.5 inch to 2.0 inch. But,for the 1.0 inch flow tube the wall effect is appreciable. The overall increase in damping is about 16% to 24% as we go from 2.5 inch to 1.0 inch flow tube at a velocity of 25 ft/sec as compared to no-flow conditions. This relatively lower increase in damping with the flow velocity may be due to larger initial damping values ($\delta_{NF}$) for 1/2 inch test rod as compared to other test rods.

Fig. 10 indicates the effect on a 5/8 inch test rod. Wall effect is small as we move from 2.5 inch to 2.0 inch flow tube; but it becomes most prominent for the 1.0 inch flow tube (55% increase in damping for a velocity of 17 ft/sec as compared to no-flow condition. This can be attributed to the fact that the initial damping values ($\delta_{NF}$) are moderate and the stiffness is of the same order as that of 1/2 inch test rod, thus the motion has more chances to be damped out with the flow velocity. Also, the damping contribution due to normal drag force for a 5/8 inch test rod will be maximum.

A general inference can be drawn that if the initial damping is small then the wall confinement will have more effect on a lower stiffness test rod to damp out the motion as the flow velocity increases.

## 3.4 R.M.S. Response at Various Flow Velocities:

### 3.4.1 Graphical Plots:

Figs. 11,12 and 13 give the wall confinement effect on the r.m.s. response of test rods as a function of mean-axial flow velocity. Plots are given on the log-log paper with r.m.s. response in Milli-volts* as ordinate and flow velocity (ft/sec) as abscissa. Here, only vertical component of the response was plotted because in almost every case it was found that the horizontal component was around 90% of the vertical component** and the horizontal component varied in the same manner with respect to flow velocity. Thus the vertical component can represent the wall effect.

### 3.4.2 Discussion:

Experimental data fit very well in the power function relationship of the type $Y = A \cdot (X)^B$, with minimum standard

---

\* Strain-Indicator Scope-Output specification is 10 Micro-Strain per Milli-volt. The gain of D.C. Amplifier is selected as 100. Thus the output is 10 Micro-Strain per 100 Milli-volts.

\*\* Typical values of horizontal and vertical components of the response are given in Appendix-3.

error. Values of exponent B were computed and are tabulated
below:

## Exponent B

| Flow tube size | 1.0 inch | 2.0 inch | 2.5 inch |
|---|---|---|---|
| Test rod size | | | |
| 3/8 inch | 2.48985 | 1.76159 | 1.52096 |
| 1/2 inch | 1.52461 | 1.27949 | 1.15267 |
| 5/8 inch | 1.87351 | 1.52034 | 1.36915 |

Power function relationship satisfied by the experi-
mental data agree with the theoretical and experimental
results of Chen and Wambsganss(21, 23). Chen(21) found the
value of exponent B in the range of 1.5 to 2.0. We can infer,
from the present experiment, that the wall confinement can
increase the exponent B in the range of 1.15 to 2.5. However,
the upper and lower bound for the exponent B will depend upon
the flow noise in the test-loop, damping, rod end support
conditions and flexural rigidity.

Wall effect for a 3/8 inch test rod is presented
in Fig. 11. R.M.S. response increases considerably even for
the confinement from 2.5 inch to 2.0 inch flow tube. Con-
finement effect for 1.2 inch size influences the response

level to a maximum value.  This is due to the fact that the stiffness of the test rod is small and a disturbance created around the test rod will become more severe after reflecting from the flow tube wall, resulting in further increase in response.

Figs. 12 and 13 represent the effect on 1/2 inch and 5/8 inch test rod.  The response level and its rate of increase is more for 5/8 inch test rod than that for 1/2 inch size, though the stiffness is large (theoretically 65%) for 5/8 inch test rod.  This is attributed to the wall confinement effect. The confinement parameter d is 25% more for 5/8 inch test rod compared to 1/2 inch rod.

### 3.4.3  Graphical Plots:

Figs. 14, 15 and 16 represent the wall effect on the r.m.s. response (vertical) as a function of flow velocity in the linear scale.  Straight lines of best fit in Figs. 11, 12 and 13 were used to represent the numerator of the ordinate denoted as $X_D$.  Denominator ($X_{LD}$) of the ordinate is the vertical response values for the largest diameter flow tube.

### 3.4.4  Discussion:

Each figure show  the wall confinement effect for various test rods on a linear scale.  These figures express the conclusions of Section 3.4.2 in a much more lucid way.

The response and its rate of increase with the flow velocity decreases with the increase in stiffness of the test rods (compare Figs. 14 and 15 or 14 and 16). But at the same time, wall confinement effect helps in building up the response and the rate of increase in response for the larger stiffness test rod (Figs. 15 and 16). In the present work, larger stiffness test rods have also the larger outer diameter (that is the greater wall confinement). It will be interesting to work on the lower stiffness with larger diameter and constant stiffness with different diameter test rods to understand the wall confinement effect in a broader sense.

## 3.5 Response Spectrum:

### 3.5.1 Graphical Plots:

Power spectral density of the test rod response is plotted for different flow velocities in Figs. 17,18,19 and 20. Here also the vertical component of the response is selected as ordinate. Frequency in Hertz is taken as abscissa in a linear scale. To measure the spectral components accurately the gain of D.C. amplifier was further increased by 5 times.

### 3.5.2 Discussion:

A glance on these plots will reveal that, apart from pump (24.2 Hz) and the line frequency noise (50 Hz), a
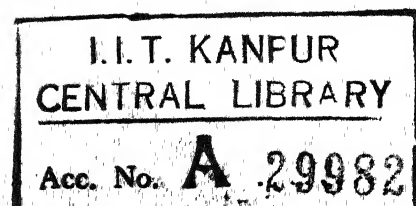
considerable amount of energy is distributed at frequencies other than the rod natural frequency. The energy distribution is mainly at the rod natural frequency for lower values of flow velocities. But at higher flow velocities the energy distribution is less at the rod natural frequency. This behavior can be due to two reasons:

1) Test rods possess high damping factor, thus the frequency-response function of the test rod will be fairly broad and will contain additional frequencies, on the both sides of fundamental frequency, with significant response.

2) The spectral energy distribution of the pressure fluctuation in the turbulent boundary layer around the test rod increases at the lower frequencies with the increase in flow velocity. This is attributed to the fact that the energy of larger eddies will be transferred to the smaller ones, due to the turbulence decay process(32).

Figs. 17 and 18 show the wall confinement effect on the power spectral distribution for the 1/ 2 inch test rod. A 25% increase in wall confinement (when the flow tube diameter is changed from 2.5 inch to 2.0 inch) increases the energy distribution at lower frequencies in a larger proportion than

its increase at the rod natural frequency. Figs. 19 and 20
display the same effect for a 3/8 inch test rod for a 50%
increase in wall confinement parameter d (when the flow tube
is changed from 2.0 inch to 1.0 inch size).

# Effect of partial filling on damping factor

|            | 1.0" ψ    | 2.0" ψ     | 2.5" ψ    |
|------------|-----------|------------|-----------|
| $\beta_{NW}$ | 0.040   | 0.0388     | 0.042     |
| d          | 0.375     | 0.1875     | 0.150     |
| ω          | 29.1 Hz   | 28.34 Hz   | 28.11 Hz  |

Test rod dia = 3/8" ∅

Wall thickness t = 0.039

2.2

1.0" ψ

1.8

2.0" ψ

2.5" ψ

1.4

$\beta_W / \beta_{NW} \longrightarrow$

1.0

0   1/4   1/2   3/4   Full

Empty
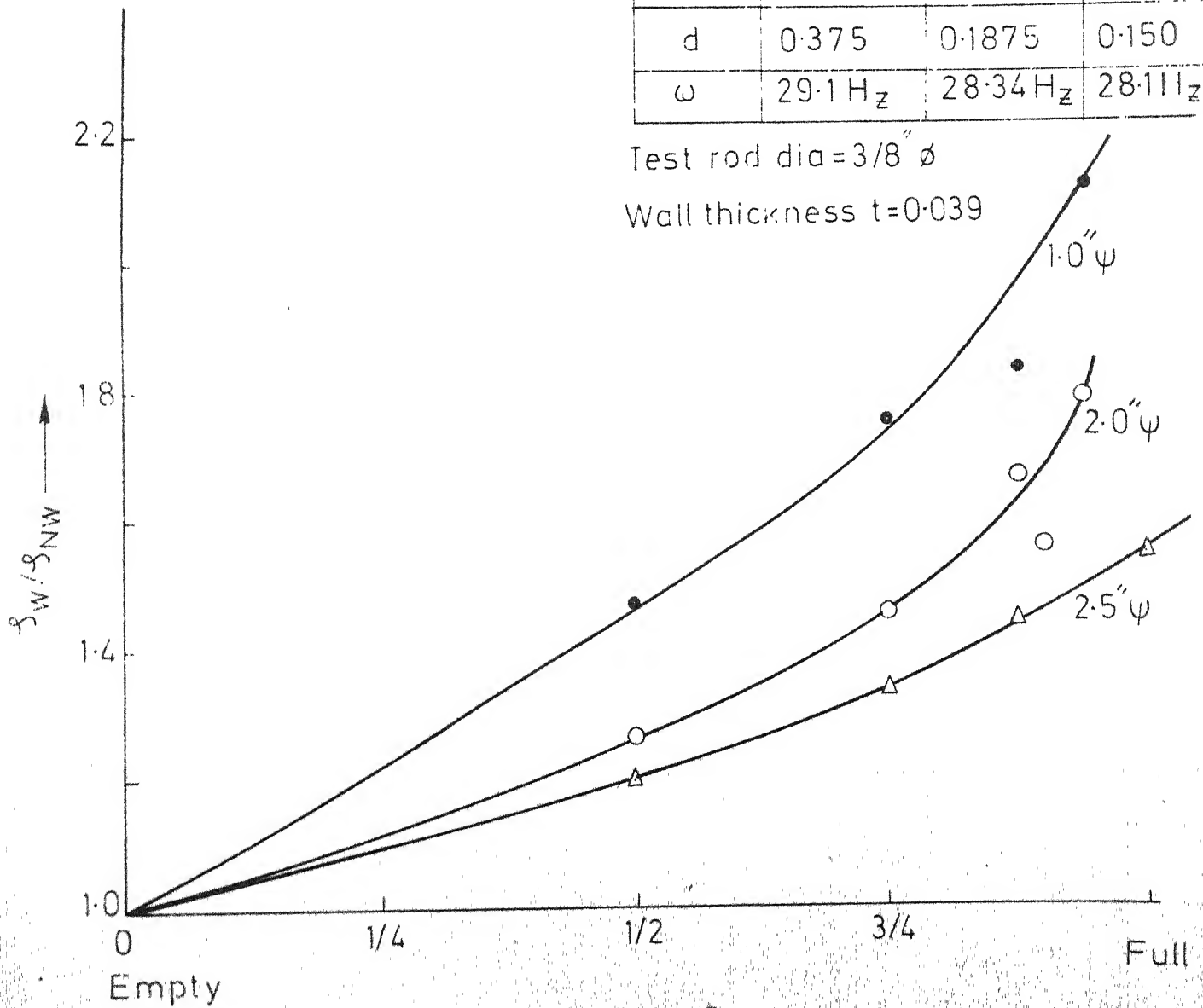
FIG. -5

# Effect of partial filling on damping factor

|  | 1·0″ψ | 2·0″ψ | 2·5″ψ |
|---|---|---|---|
| $\zeta_{NW}$ | 0·0731 | 0·084 | 0·074 |
| d | 0·500 | 0·250 | 0·200 |
| ω | 31·83 Hz | 31·57 Hz | 32·1 Hz |

Test rod dia = 1/2″ φ

Wall thickness t=0·0595″
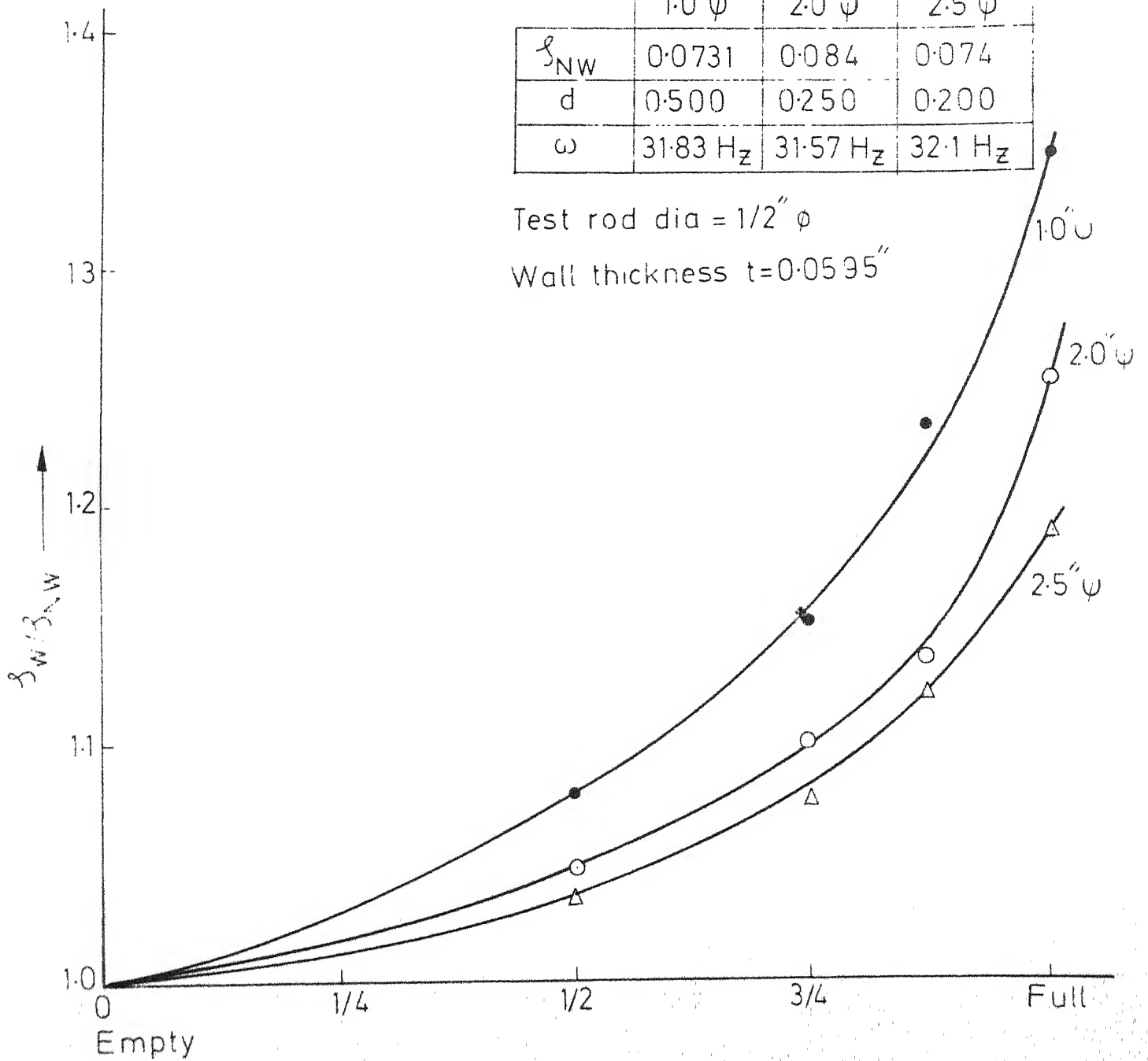


FIG·-6

# Effect of partial filling on damping factor

|  | 1·0″ψ | 2·0″ψ | 2·5″ψ |
|---|---|---|---|
| $\delta_{NW}$ | 0·058 | 0·0628 | 0·064 |
| d | 0·625 | 0·3125 | 0·250 |
| ω | 37·2 Hz | 36·4 Hz | 36·15 Hz |

Test rod dia = 5/8″ ⌀

Wall thickness t = 0·049
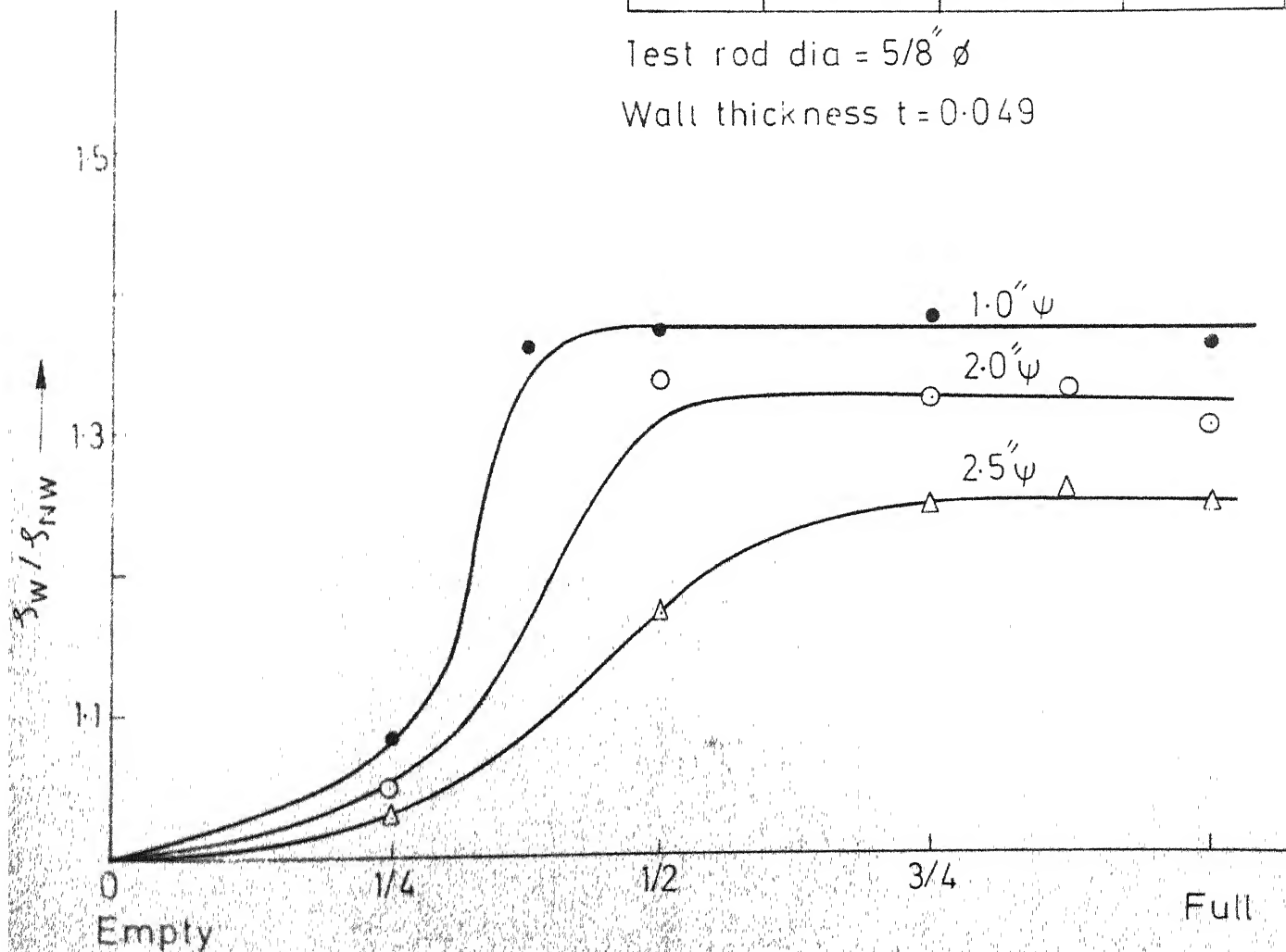


FIG-7

# Damping factor Vs flow velocity



|  | 1.0 ψ | 2.0 ψ | 2.5 ψ |
|---|---|---|---|
| $\beta_{NF}$ | 0.0600 | 0.0848 | 0.0651 |
| 1 | 0.375 | 0.1875 | 0150 |

Test rod dia = 3/8″ φ
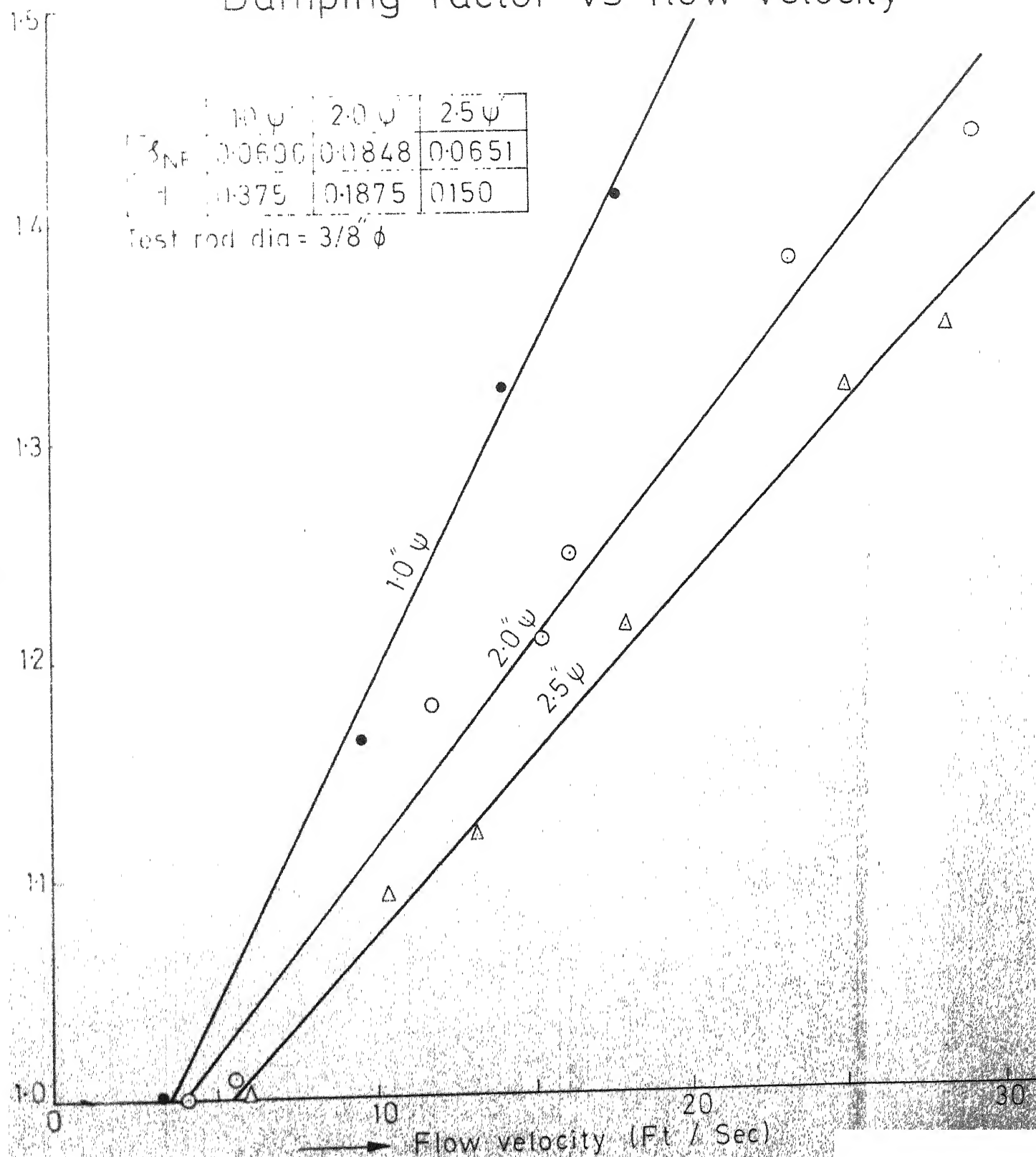
FIG-8

Damping factor Vs flow velocity

| | 1·0″ ψ | 2·0″ ψ | 2·5″ ψ |
|---|---|---|---|
| $\delta_{NF}$ | 0·0985 | 0·1056 | 0·0834 |
| d | 0·500 | 0·250 | 0·200 |

Test rod dia = 1/2″ φ

FIG.-9

# Damping factor Vs flow velocity

| $\delta_{NF}$ | 1.0" $\psi$ | 2.0" $\psi$ | 2.5 $\psi$ |
|---|---|---|---|
| $\delta_{NF}$ | 0.0795 | 0.0822 | 0.080 |
| d | 0.625 | 0.3125 | 0.250 |

Test rod dia = 5/8" ø

$\delta_F/\delta_{NF}$

Flow velocity (Ft/Sec)
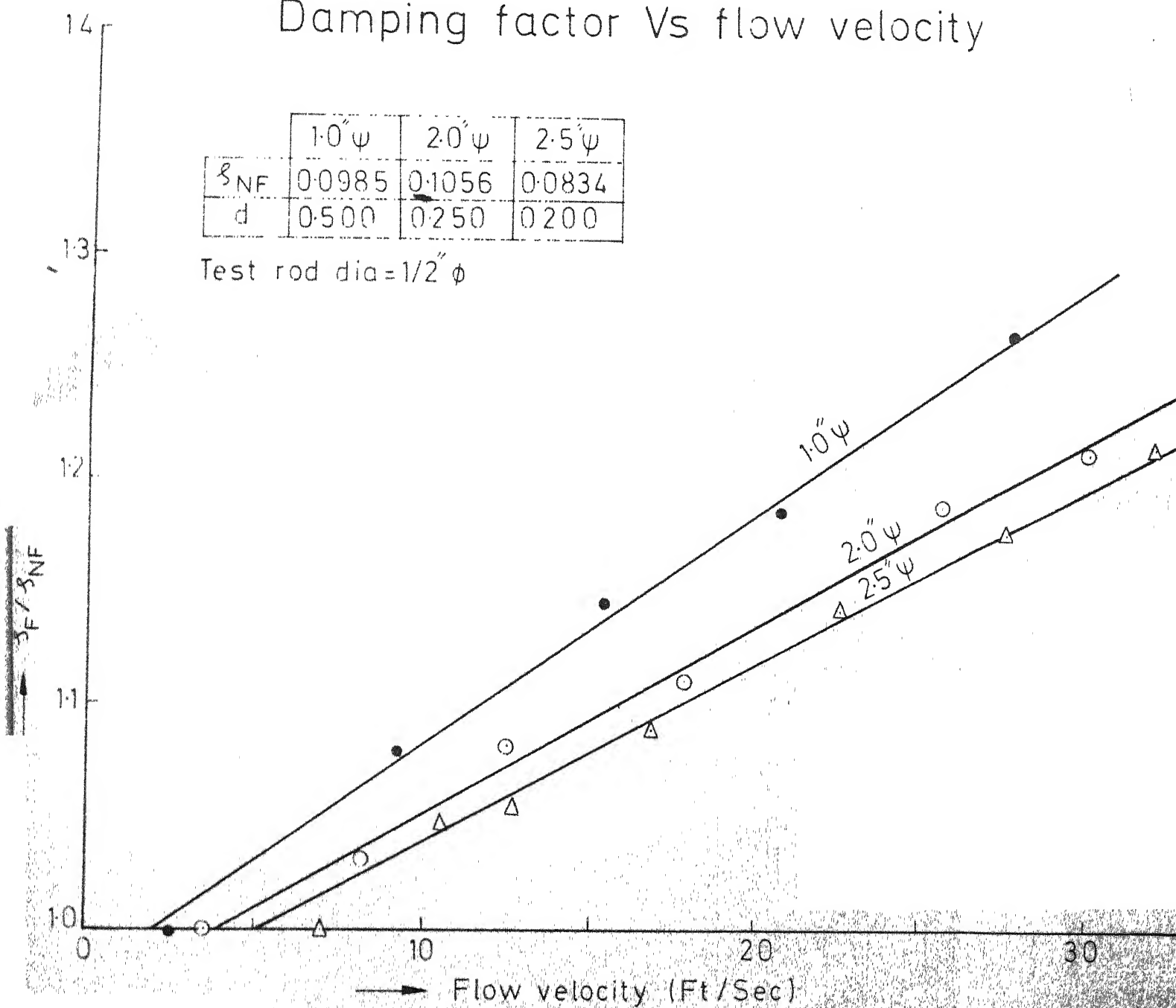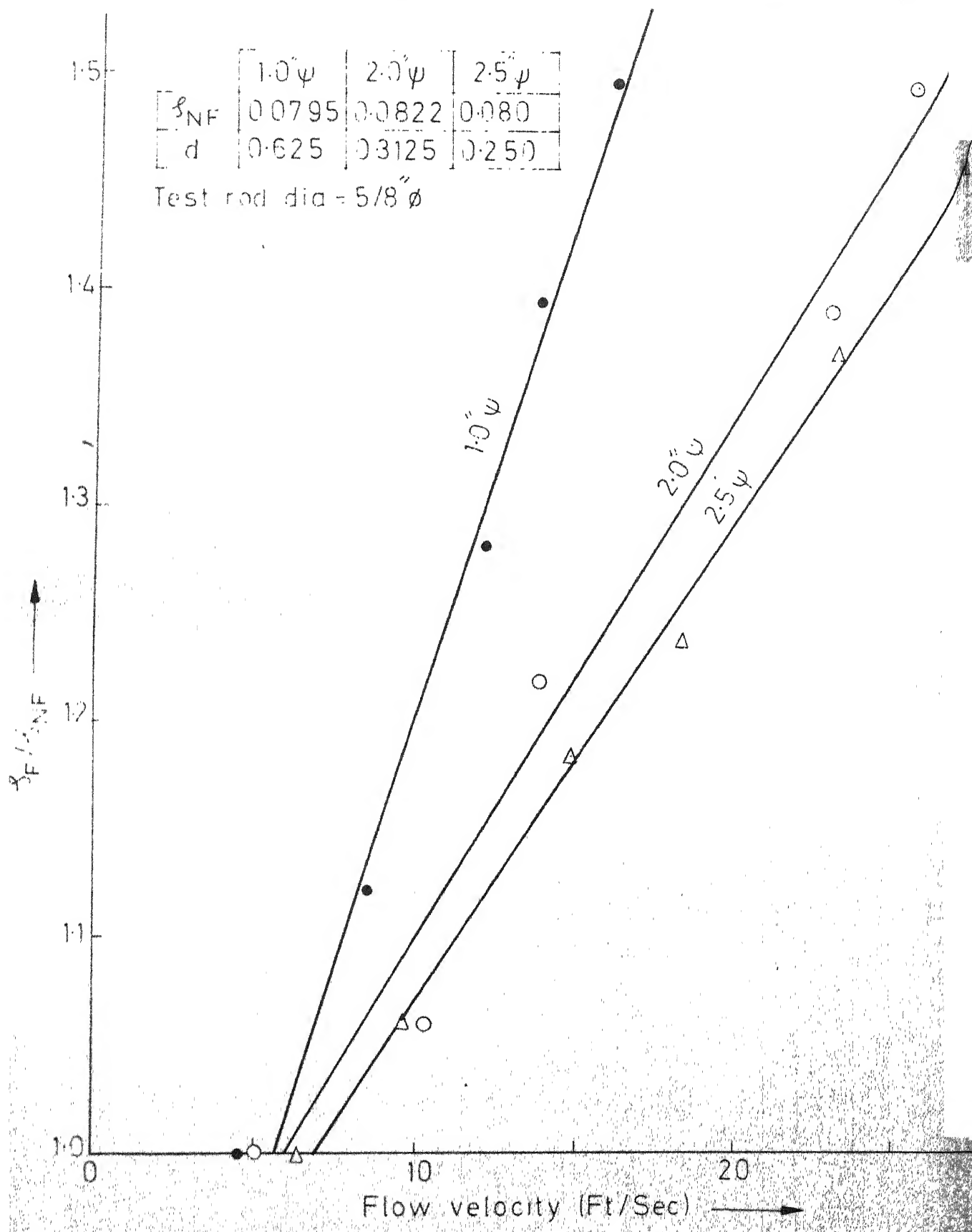
FIG-10
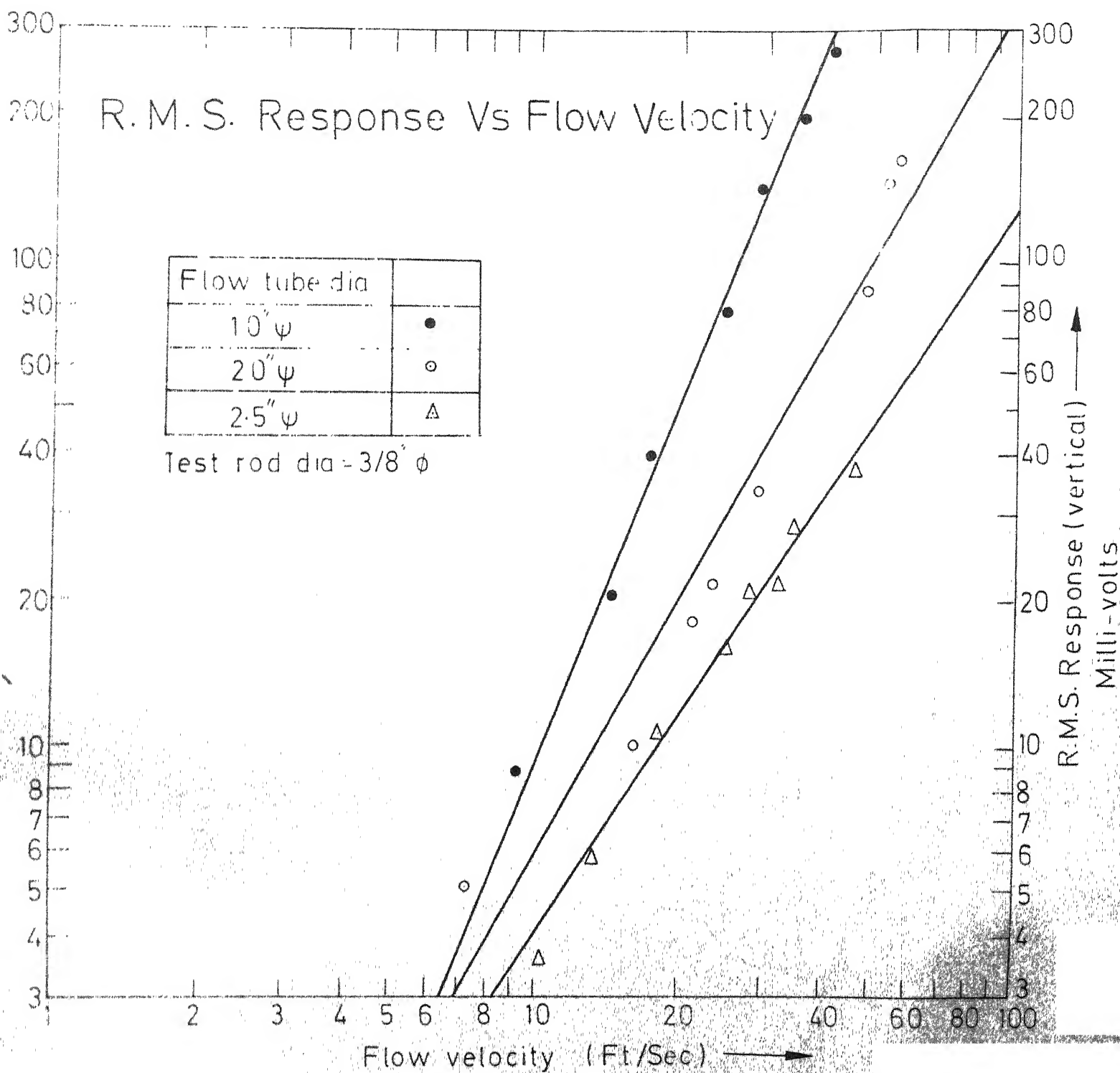
FIG.-11

R.M.S. Response Vs Flow Velocity
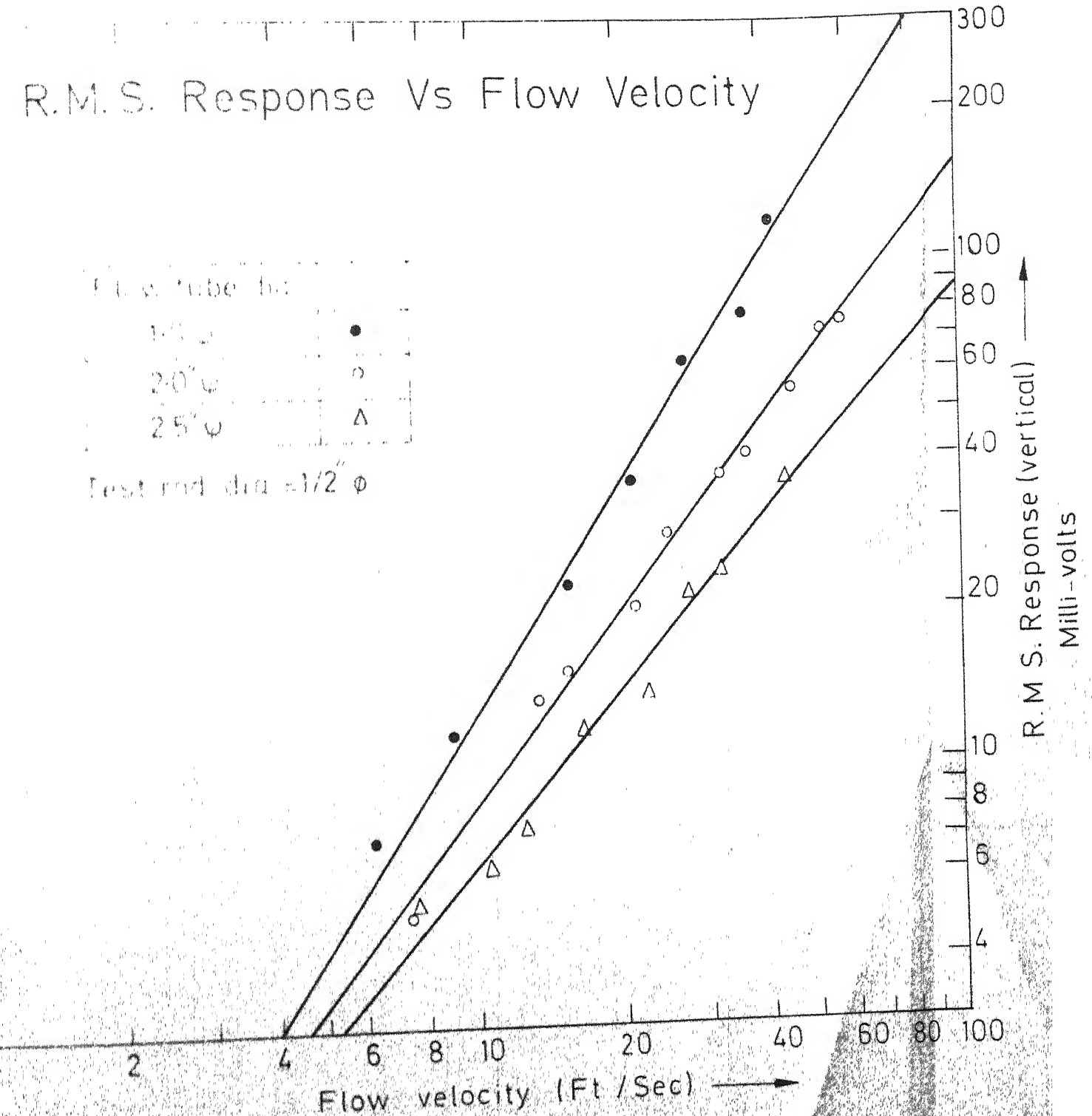
FIG.-12

FIG.-13

# Wall effect on the response



Test rod dia = 3/8" $\phi$

Axis labels:
- Y-axis: $x_D / x_{LD}$
- X-axis: Flow velocity (Ft/Sec)

Curve labels: 1.0" $\psi$, 2.0" $\psi$, 2.5" $\psi$

FIG.14

# Wall effect on the response



Test rod dia -1/2″ φ

1·0″ ψ

2·0″ ψ

2·5″ ψ

$\overline{x_D / x_{LD}}$ ⟶
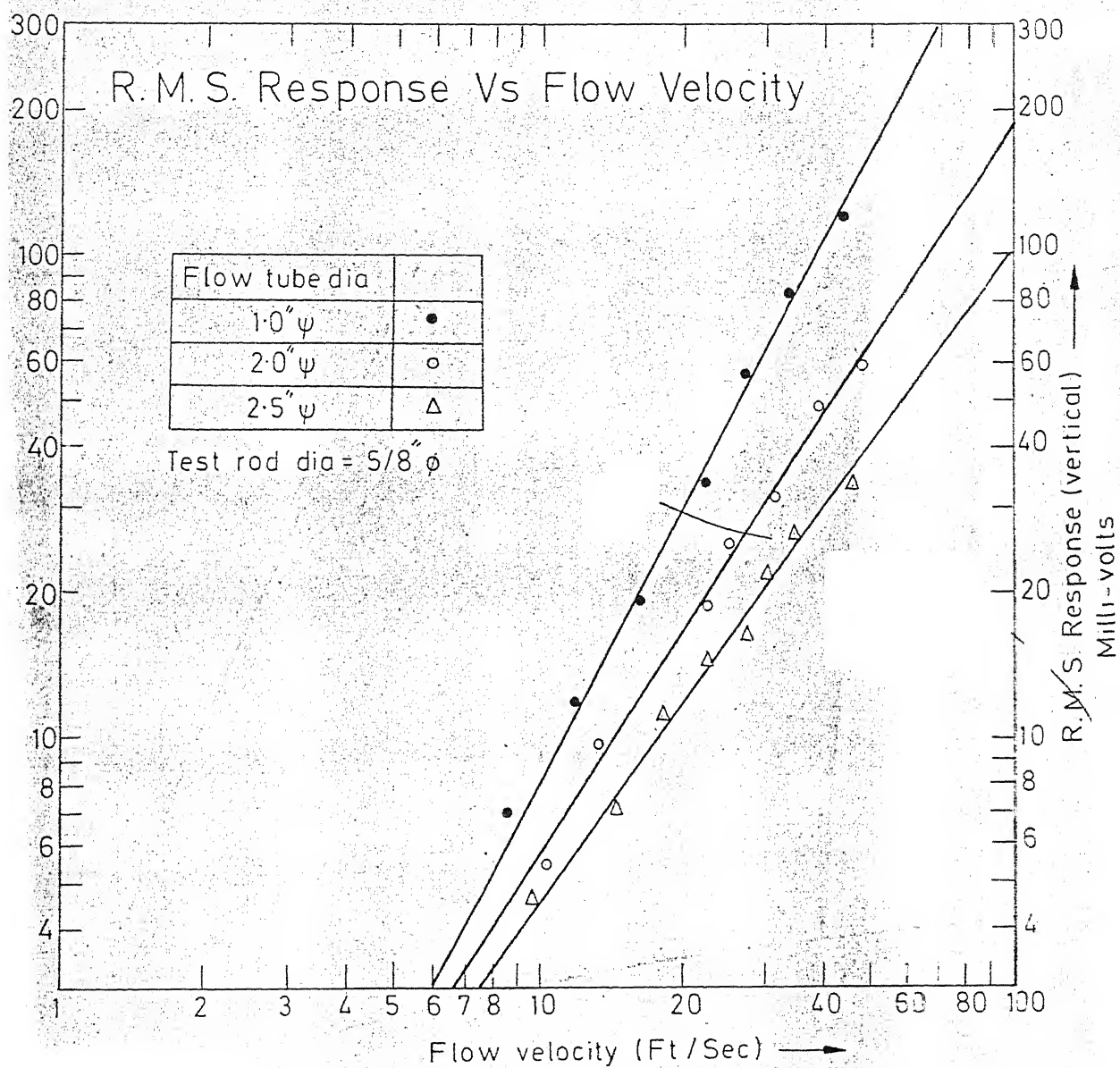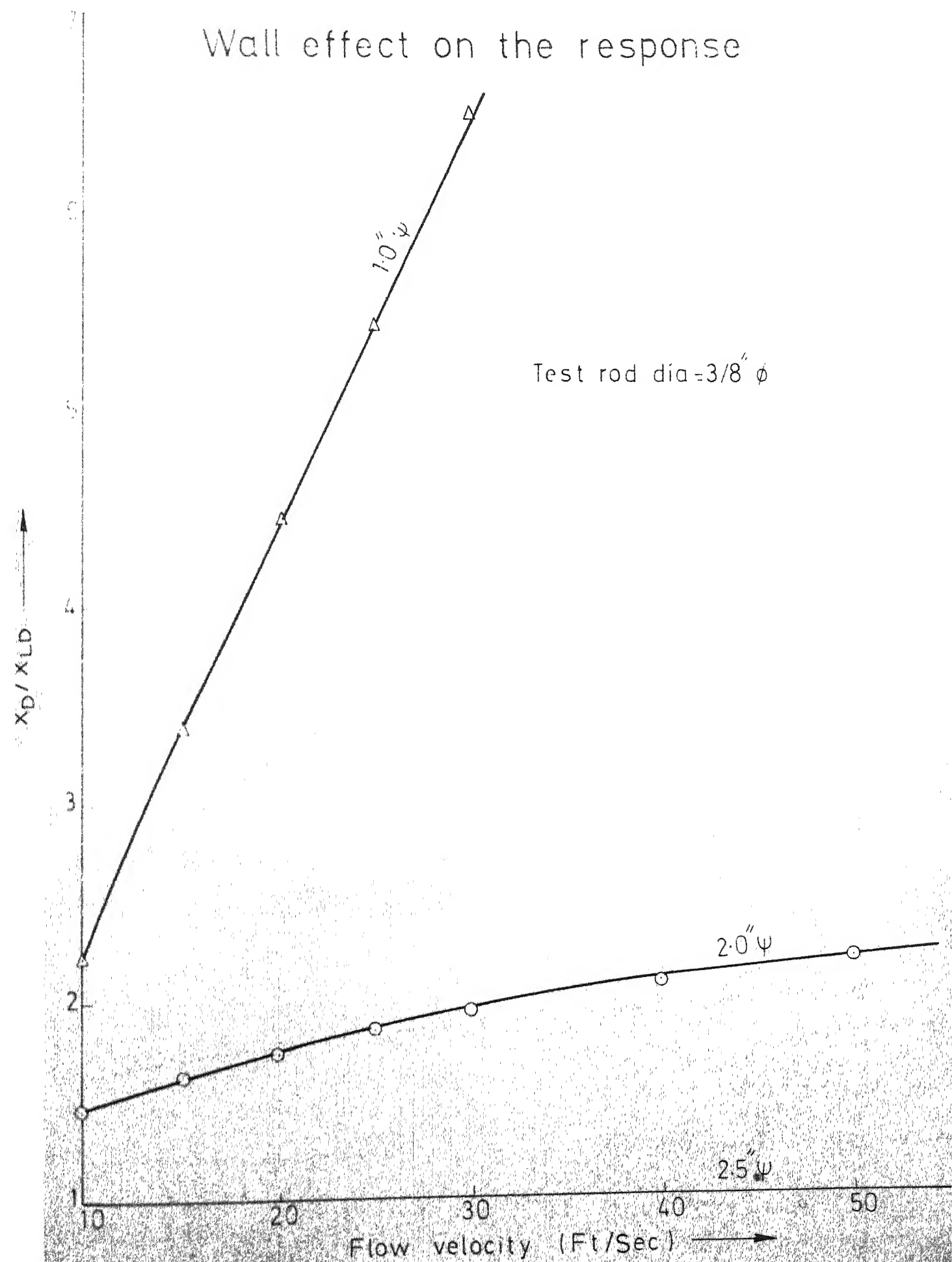
Flow velocity (Ft/Sec) ⟶
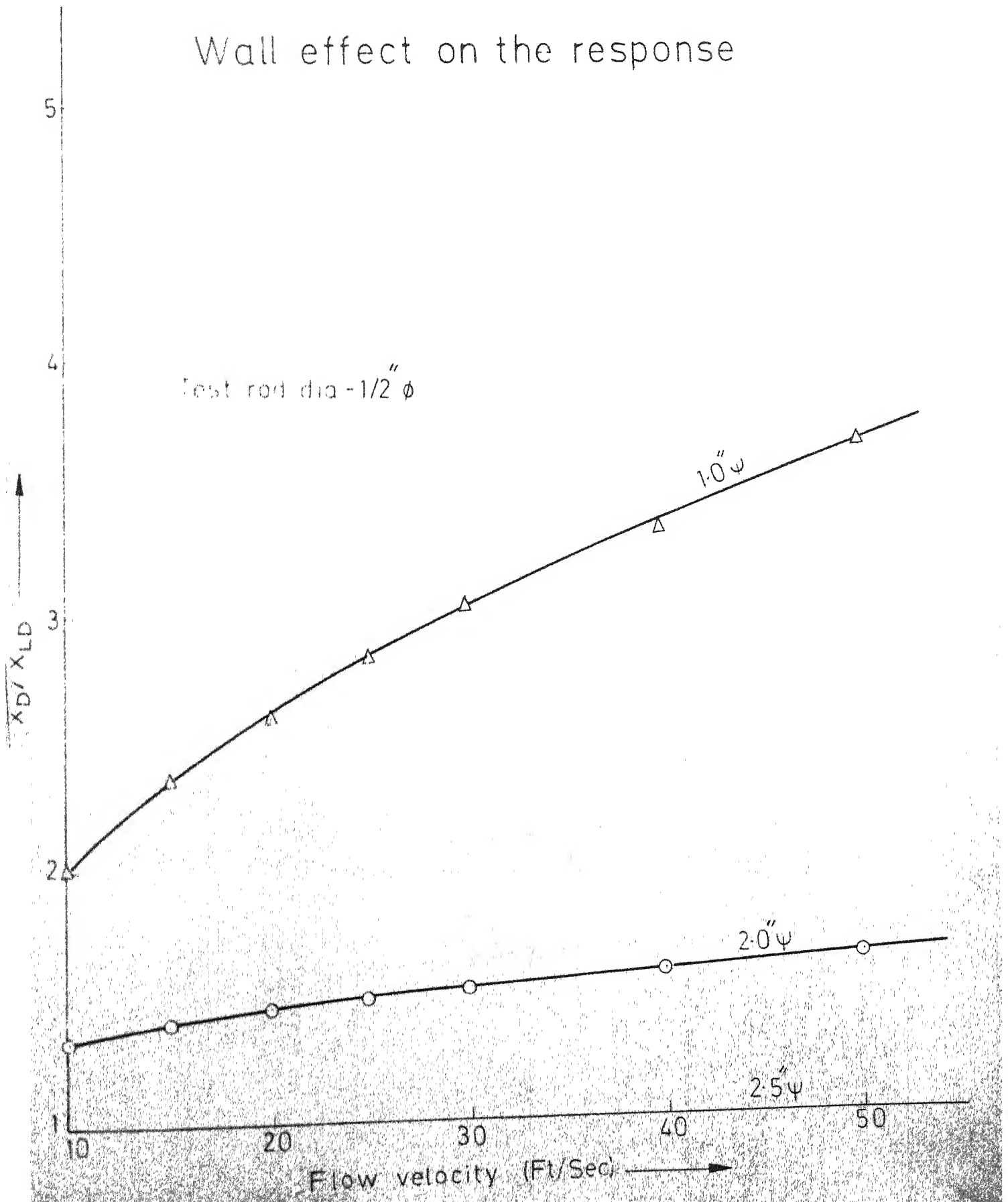
FIG -15

Wall effect on the response

Test rod dia = 5/8″ φ

FIG. 16

# Response Spectrum



| Flow velocity | ft/sec |
|:---:|:---:|
| 1 | 7·365 |
| 2 | 21·1 |
| 3 | 32·55 |
| 4 | 52·8 |

Test rod dia = 1/2″ $\phi$

Flow tube dia = 2·0″ $\psi$
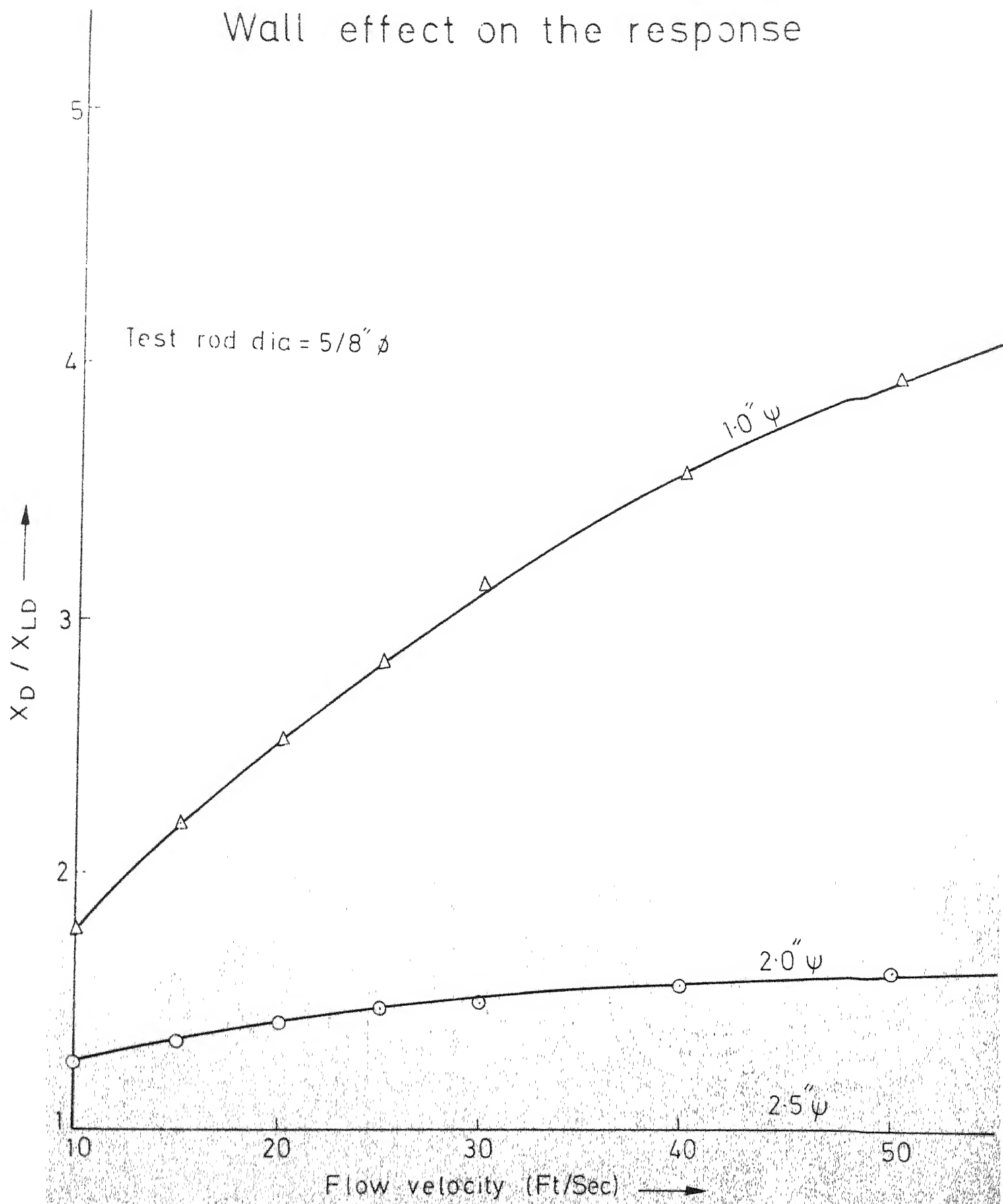
Rod natural frequency = 31·57 Hz
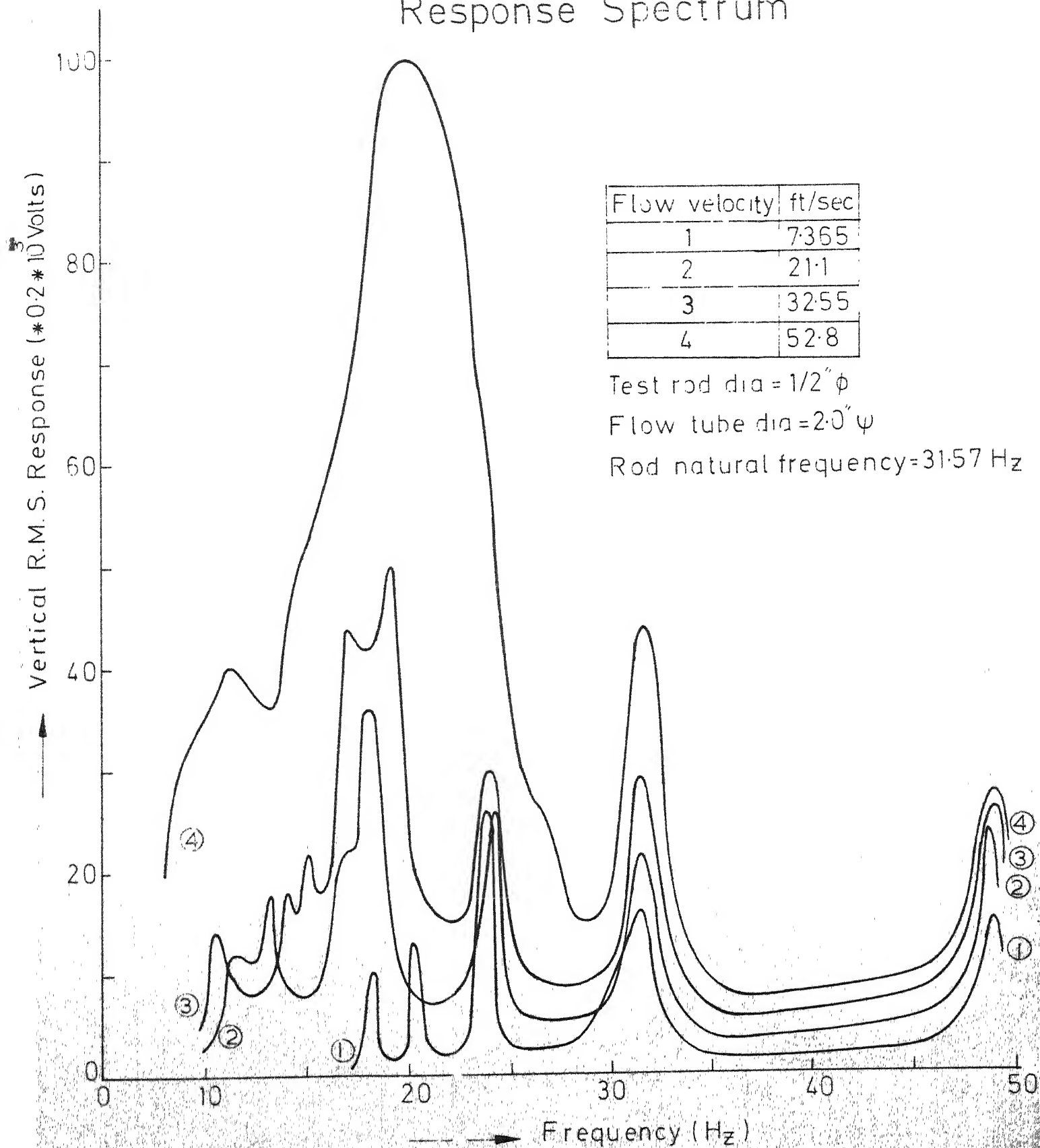
FIG. -17

# Response Spectrum



| Flow velocity | ft/sec |
|:---:|:---:|
| 1 | 7·52 |
| 2 | 10·4 |
| 3 | 18·6 |
| 4 | 31·78 |
| 5 | 40·45 |

Test rod dia = 1/2″ φ

Flow tube dia = 2·5″ ψ

Rod natural frequency = 32·8 H$_z$
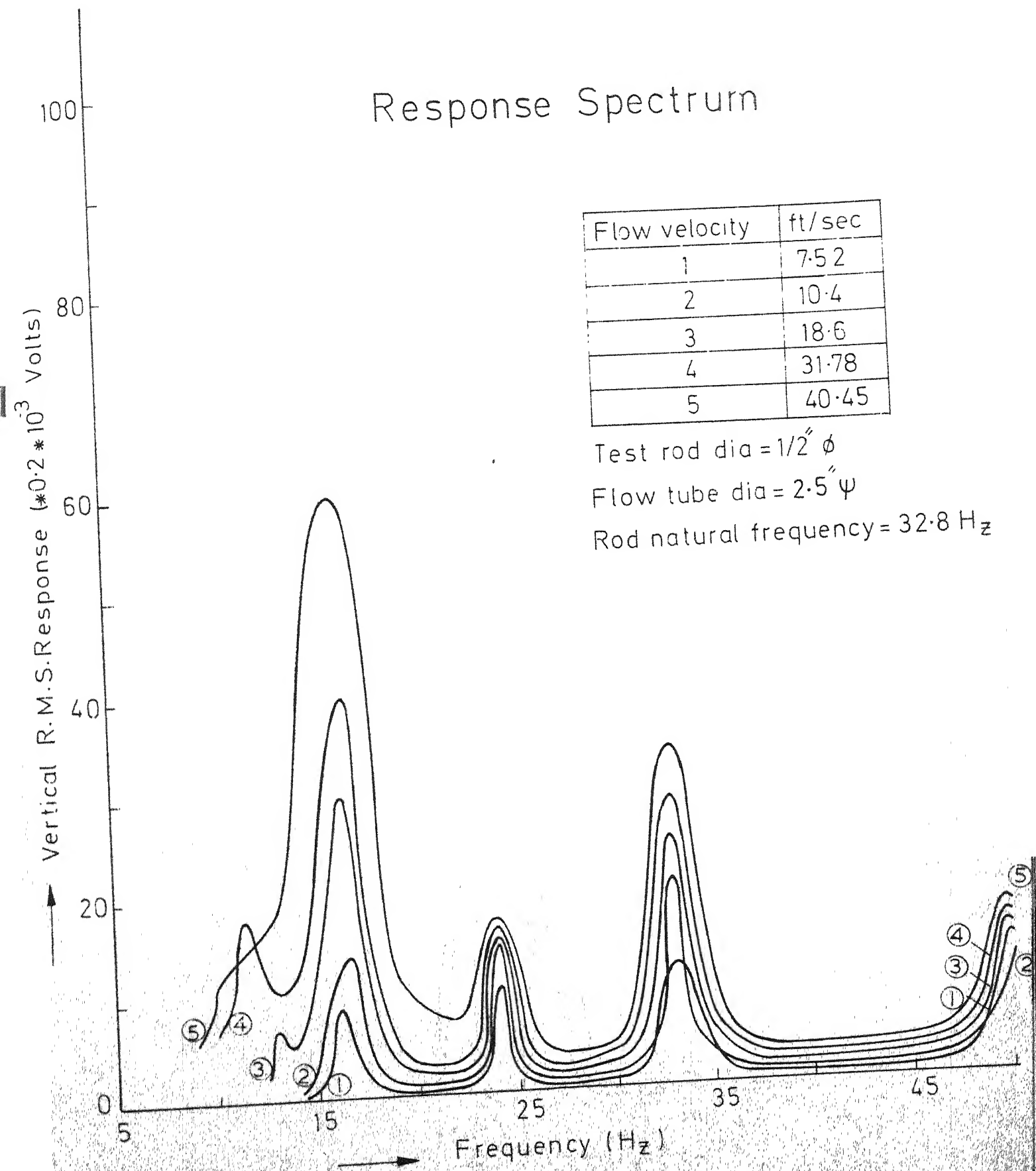
Vertical R.M.S. Response (*0·2 *10$^{-3}$ Volts)

Frequency (H$_z$)

FIG.-18

# Response Spectrum

| Flow velocity | ft / sec |
|:---:|:---:|
| 1 | 5·60 |
| 2 | 15·22 |
| 3 | 18 20 |
| 4 | 22·32 |

Test rod dia = 3/8" φ

Flow tube dia = 2·0" ψ

Rod natural frequency = 28·34 Hz



FIG. -19

# Response Spectrum



| Flow velocity | ft/sec |
|---|---|
| 1 | 3·385 |
| 2 | 8·13 |
| 3 | 13 47 |

Test rod dia =3/6 $\phi$

Flow tube dia =1·0" $\psi$

Rod natural frequency = 29·1 Hz
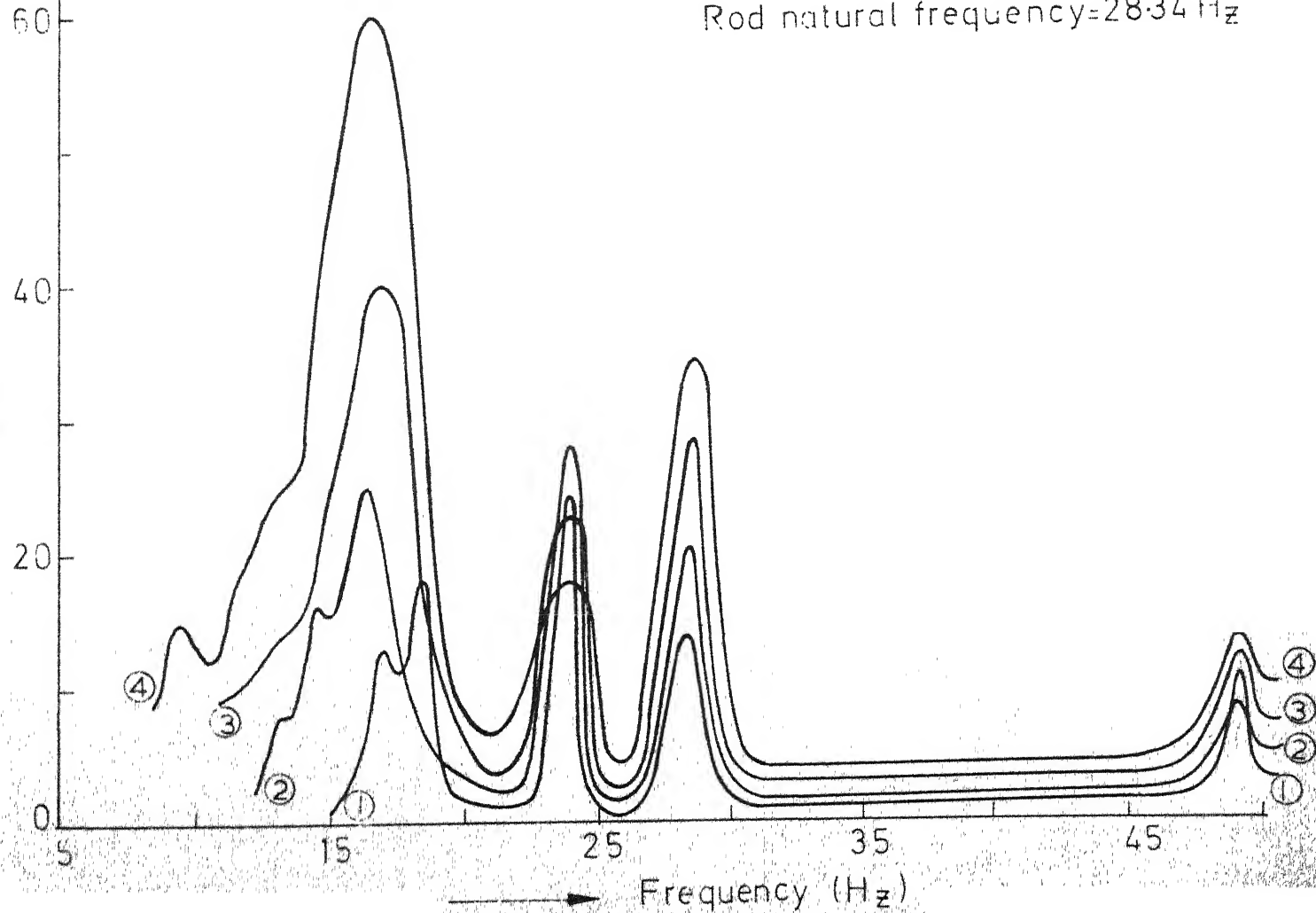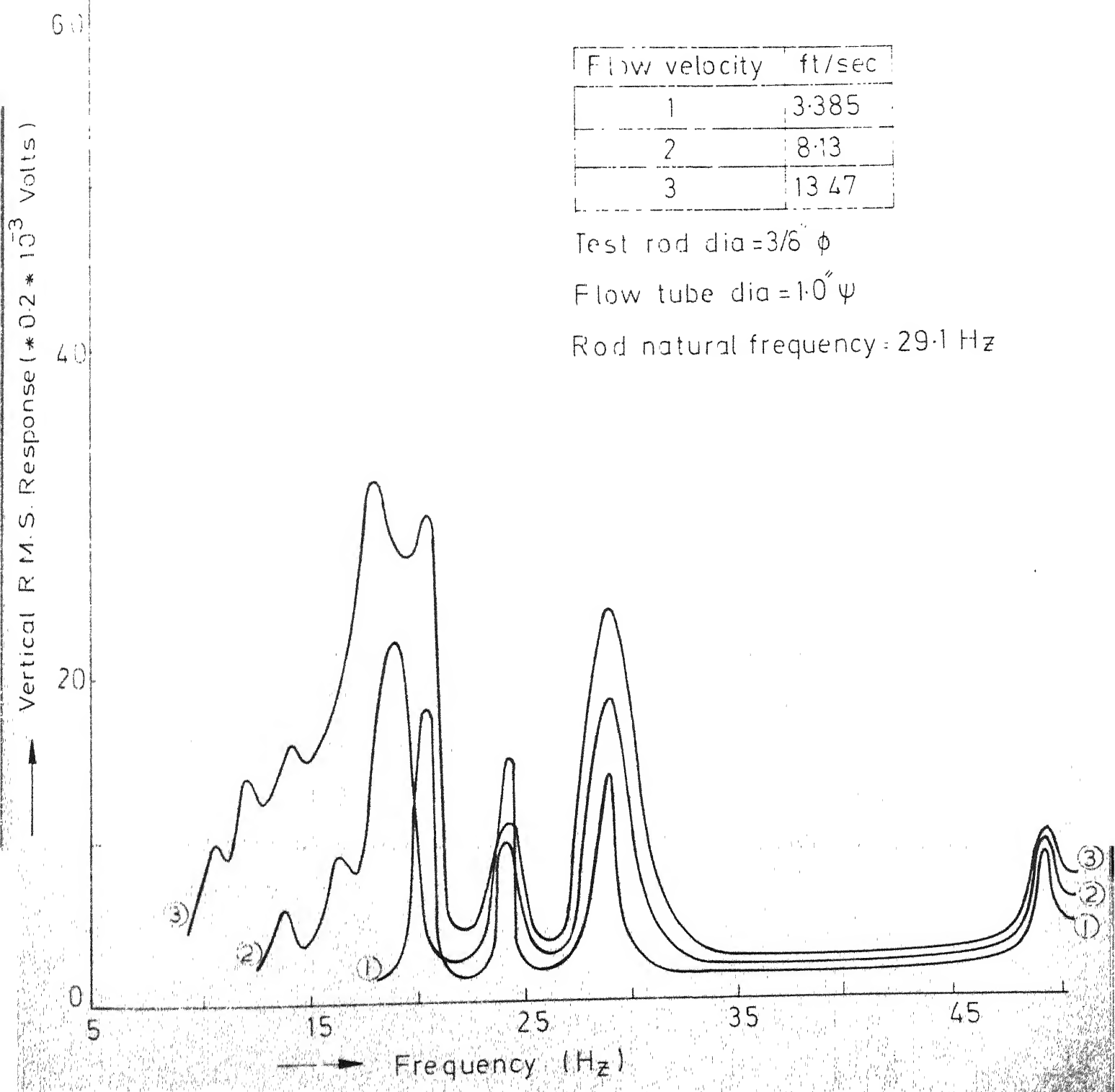
FIG.-20

# CHAPTER-IV

# CONCLUSIONS AND SCOPE FOR FUTURE WORK

## 4.1 Conclusions:

### 4.1.1 Effect of Water Level on the Damping:

(1) Damping factor increases with the water level; its rate of increase, decreases for the stiffer test rod.

(2) Rate of increase in damping and wall confinement effect will be more, if the initial damping of the test rod (with no-water) is small.

(3) Damping contribution due to normal drag force will be more for the larger diameter test rod and will result in an increase in damping upto 1/2 water level. After that, it becomes more or less constant with the increase in water level in the flow tube.

### 4.1.2. Effect of Flow Velocity on the Damping:

(1) Damping increases with the flow velocity and follow a straight line fit.

(2) For the lower stiffness test rod, wall effect is prominent even at lower values of wall confinement para-meter d.

(3) If the damping at the initial flow velocity is large, the slope of damping line is small and wall confinement has not much effect on the increase in damping.

(4) Natural frequency of damped oscillations remains almost constant for the moderate velocity range (0 to 30 ft/sec) and also the wall confinement has very little effect on it.

(5) Contribution due to normal drag force, with the increase in flow velocity, helps in raising up the damping values for the larger diameter test rod.

### 4.1.3  Effect on the R.M.S. Response:

(1) R.M.S. response increases with the flow velocity and follow a power function relationship.  The exponent of the power function relationship ranges between 2.5 to 1.15 in the present study.  Exponent values will depend on the flow noise, damping, rod end-support conditions and flexural rigidity of the test rods.

(2) Response increases with the wall confinement for the same test rod in various flow tubes.  Wall confinement has greater effect on the response level, if the exponent of power function relationship is large for the test rod in the largest diameter flow tube.

(3) If the stiffness of two test rods are not far apart, the response level will be mainly governed by the wall confinement parameter d.

### 4.1.4  Effect on the Power Spectral Density:

(1)  At lower flow velocities, energy is mainly distributed around the rod natural frequency and some energy is available at lower frequencies.  But at higher flow velocities, most of the energy density is shifted towards the lower frequencies.  This is possibly due to large damping of the test rod (wide frequency-response function) and the turbulence decay process of the larger eddies (resulting in shifting of the energy density of the forcing function to lower frequencies)

(2)  Wall confinement tends to further increase  the energy density at lower frequencies as compared to rod fundamental frequency.

### 4.2  Scope for Future Work:

In the present work, the wall confinement effect was studied for the test rods having larger stiffness for larger diameter.  These studies resulted in high values of response for smallest stiffness test rod and thereby giving the impression of larger wall effect, though the wall confinement parameter d is small as compared to larger diameter test rods.  It will be worthwhile to work on the test rods having lower stiffness with larger diameter ( to know that how the disturbances help in the growth of response, as the wall confinement increases) and constant stiffness with different diameter test rods (to investigate the absolute effect of wall confinement on the response level).

Wall confinement effect can be understood in a better way, if we have the knowledge of the forcing function distribution (random pressure measurement in the turbulent boundary layer around the test rod) and the frequency-response function for the test rods (mounted in the external flow tube).

The response sensing device should be such that it should not disturb the flow at the point where it is attached to the test rod (unlike the strain gages used in the present study). One of the solution is to use miniature piezoelectric transducer flush mounted in a cavity in the test rod wall thickness.

Above stated is the work mainly connected with the vibrational aspect of the present problem. Deep understanding of the problem can only be achieved by studying also the fluid mechanics aspect. It will be interesting to know that how the flow disturbances are originated, grow-up and cause the test rod to vibrate; how the vibrating test rod affects the disturbances producing it and what is its consequence on the vibration amplitude when the wall confinement is increased. This will further require to understand the mechanism of energy transfer from flowing fluid to the solid.

REFERENCES

1. Ashley, H. and Haviland, G., "Bending Vibrations of a Pipe Line Containing Flowing Fluid", Trans. ASME, J. of Applied Mechanics, Vol. 17, 1950, pp. 229-232.

2. Williams, M.M.R., "Reactivity Changes Due to the Random Vibration of Control Rods and Fuel Elements", Nucl. Sci. & Engg., Vol. 40(1), 1970, pp. 144-150.

3. Burgreen, D.; Byrnes, J.J. and Beneforado, D.M., "Vibration of Rods Induced by Water in Parallel Flow", Trans. ASME, 80(5), 1958, pp. 991-1003.

4. Hyndman, R.W. et. al., "EBR-II Self-Excited Oscillations", Trans. Amer. Nucl. Soc., 8(2), 1965, pp. 590.

5. Dalke, C.A., "Elimination of Hydraulically Induced Core Vibrations of General Electric Test Reactor", Trans. Amer. Nucl. Soc., 8 (Suppl.), 1965, pp. 2.

6. Riesland, J.I. and Gustafson, E.A., "Work Performed on Fuel Channels and the Core Support Plate at Big Rock Point Nuclear Power Plant", Trans. Amer. Nucl. Soc., 8 (Suppl.), 1965, pp. 5-9.

7. Reed, G.A., "Major Operating and Refuelling Problems at the Yankee Atomic Electric Company Rowe Power Plant", Trans. Amer. Nucl. Soc., 8 (Suppl.), 1965, pp. 28.

8.      Heffner, R.E., "Six-Years Operating Experience
        with PWR Plant Components", Trans. Amer.
        Nucl. Soc., 8 (Suppl.), 1965, pp. 29-30.

9.      Oak Ridge National Laboratory, "Molten Salt
        Reactor Program Semiannual Progress
        Report for Period Ending Jan. 31, 1964",
        USAEC Report ORNL-3626, July 1964.

10.     Paidoussis, M.P., "The Amplitude of Fluid
        Induced Vibrations of Cylinders in Axial
        Flow", Canadian Report AECL - 2225,March
        1965.

11.     Paidoussis, M.P., "Vibration of Flexible Cylinders
        with Supported Ends, Induced by Axial Flow",
        Proc. Inst. Mech. Engrs., 180 (Part 3J),
        1965-66.

12.     Lighthill, M.J.,"Note on Swimming of Slender
        Fish", J. Fluid Mech. 9(2), 1960, pp. 305-
        .317.

13.     Paidousis, M.P., "Dynamics of Flexible Slender
        Cylinders in Axial Flow Part I:Theory",
        J. Fluid Mech., 26(Pt. 4), 1966, pp. 717-
        736.

14.     Paidoussis, M.P., "Dynamics of Flexible Slender
        Cylinders in Axial Flow, Part II:
        Experiment", J. Fluid Mech., 26(Pt.4),
        1966, pp. 737-751.

15.     Paidoussis, M.P.,and Sharp, F.L., "An Experimen-
        tal Study of the Vibration of Flexible
        Cylinders Induced by Nominally Axial Flow",
        CRNL-76, Dec. 1967.

16.     Reavis, J.R., "WVI - Westing House Vibration
        Correlation for Maximum Fuel Element
        Displacement in Parallel Turbulent Flow,"
        Paper Presented at 13th. Annual Meeting
        Amer. Nucl. Soc., June 1967. Also Published
        in Nucl. Sci. Engg., 38(1), 1969, pp. 63-69.

17.     Gorman, D.J., "The Role of Turbulence in the
            Vibration of Reactor Fuel Elements in
            Liquid Flow", Report AECL-3371, May 1969.

18.     Gorman, D.J., "An Analytical and Experimental
            Investigation of the Vibration of Cylin-
            drical Reactor Fuel Elements in Two-Phase
            Parallel Flow", Report CRNL-339, Aug. 1969.
            Also Published in Nucl. Sci. Engg., 44,
            1971, pp. 277-290.

19.     Bakewell,Jr.,H.P., "Turbulent Wall Pressure
            Fluctuations on a Body of Revolution",
            J. Acoust. Soc. Am., 43(6), 1968, pp.
            1358-1363.

20.     Gorman, D.J., "Vibration of a Simulated Fuel Rod
            Induced by Two-Phase Flow in a Seven-Rod
            Bundle", Report CRNL-409, Jan. 1970.

21.     Chen, S.S. and Wambasganss Jr., M.W., "Response
            of a Flexible Rod to Near-Field Flow Noise,"
            Proc. Conf. on Flow Induced Vibrations in
            Reactor System Components, Argonne, Illinois,
            May 14-15, 1970, ANL-7685, pp. 5-31.

22.     Wambsganss Jr., M.W. and Zaleski, P.L., "Measure-
            ment, Interpretation and Characterization
            of Near-Field Flow Noise", Report ANL-7685,
            May 1970, pp. 112-140.

23.     Chen, S.S. and Wambsganss Jr., M.W., "Parallel
            Flow Induced Vibration of Fuel Rods",
            Nucl. Engg. Design, 18, 1972, pp. 253-278.

24.     Corocos, G.M., "Resolution of Pressure in Turbu-
            lence", J. Acoust. Soc. Am., Vol. 35, 1963,
            pp. 192-199.

25.     Clinch, J.M., "Measurement of the Wall Pressure
            Field at the Surface of a Smooth-Walled
            Pipe Containing Turbulent Water Flow",
            J. Sound and Vibration, Vol. 9, 1969,
            pp. 398-419.

26.      Willmarth, W.W. and Wooldridge, C.E., "Measurements of the Fluctuating Pressure at the Wall Beneath a Thick Turbulent Boundary Layer", J. Fluid Mech., Vol. 14, Part 2, 1962, pp. 187-210.

27.      Wambsganss Jr., M.W., "Vibration of Reactor Core Components", Reactor-Fuel Process Technol., Vol. 10, No. 3, 1967, pp. 208-219.

28.      Paidoussis, M.P., "An Experimental Study of Vibration of Flexible Cylinders Induced by Nominally Axial Flow", Nucl. Sci. Engg., Vol. 35, 1969, pp. 127-138.

29.      Burgreen, "Effect of End-Fixity on the Vibration of Rods", J. Eng. Mech. Div., Oct. 1958, 1791.

30.      Chen, S.S. and Rosenberg, G.S., "Vibration and Stability of a Tube Conveying Fluid", Argonne National Lab. Report ANL-7762, March 1971.

31.      Wambsganss Jr., M.W. ; Bores, B.L. and Rosenberg, G.S., "Method for Identifying and Evaluating Linear Damping Models in Beam Vibrations", ANL-7292, April 1967.

32.      Chen, Y.N., "Turbulence Induced Instability of Fuel Rods in Parallel Flow", Sulzer Technical Review, Research No., 1970, pp. 72-84.

33.      Taylor, G.I., "Analysis of the Swimming of Long and Narrow Animals", Proc. Royal Soc. (London), A214, 1952, pp. 158-183.

34.      Paidoussis, M.P., "Dynamics of Cylindrical Structure Subjected to Axial Flow", J. Sound & Vib., 29(3), 1973, pp. 365-385.

35.      Wambsganss Jr., M.W. and Zaleski, P.L., "Flow-Velocity-Dependence of Damping in Parallel-Flow-Induced Vibration", Trans. Am. Nucl. Soc., 12 (2), pp. 839-840, 1969.

BIBLIOGRAPHY

1.    Skaardal, R.C., "Flow-Induced Vibrations",
         Power Reactor Technol., 8(4), Fall 1965,
         pp. 273-275.


2.    "Action on Reactor Projects Undergoing Regulatory
         Review", Nucl. Safety, 6(2), Winter 1964-65,
         pp. 222-223.


3.    "Thermal Shield Vibration at Big Rock Point",
         Nucleonics, 24(5), May 1966, pp. 64-65.


4.    Martens, F.H., "Design Foresight Can Simplify
         Reactor Modification", Power Reactor
         Technol., 9(2), Spring 1966, pp. 74-79.


5.    Bierman, G.F. and Miller, W.J.,"Nuclear Plant
         Performance - Good and getting Better",
         Power Reactor Technol., 9(3), Summer 1966,
         pp. 110-122.


6.    Shields, C.M. and Savannah, N.S., "Fuel Design
         and Development Program - Fuel Rod Vibra-
         tion", USAEC Report GEAP-3583, General
         Electric Company, Atomic Power Equipment
         Department, Nov. 1, 1960.


7.    Quinn, E.P., "Vibration of Fuel Rods in Parallel
         Flow," USAEC Report GEAP - 4059, July 1962.


8.    Pavlica, R.T. and Marshall, R.C., "Vibration of
         Fuel Assemblies in Parallel Flow", Trans.
         Amer. Nucl. Soc., 8(2), 1965, pp. 599-600.

9. Quinn, E.P., "Vibration of SEFOR Fuel Rods in Parallel Flow", USAEC Report GEAP-4966, Sept. 1965.

10. Pavlica, R.T. and Marshall, R.C., "An Experimental Study of Fuel Assembly Vibrations Induced by Coolant Flow", Nucl. Engg. Design, 4, 1966, pp. 54-60.

11. Roström, K.G. and Andersson, N., "Boiler Element for Marviken, Vibration Test with One Rod", Swedish Report RPL-724, 1964.

12. Roström, K.G., "Super Heater Element for Marviken, Vibration Test with One Rod," Swedish Report RPL-725, 1964.

13. Rostrom, K.G., "Seven-Rod Fuel Element Vibration Test", Swedish Report RPL - 726, 1964.

14. Societe Grenobloise d'Etude et d'Application Hydrauliques, "Study of Vibrations and Load Losses in Tubular Clusters", Special Report No. 3, USAEC-Euratom Report EURAEC - 288, March 1962.

15. Basile, D.; Faure, J. and Ohlmer, E., "Experimental Study on the Vibrations of Various Fuel Rod Models in Parallel Flow", Nucl. Engg. Design, 7, 1968, pp. 517-534.

16. Paidoussis, M.P., "Vibration of Cylindrical Structures Induced by Axial Flow", ASME/DED Vib. Conf., Cincinnati (U.S.A.), 1973.

## APPENDIX-1

### Equation of Motion as Obtained by Chen & Wambsganss (23):

An small element $\delta x$ of the rod in axial flow, with velocity V, was considered to be acted upon by axial tension T, shear force Q, bending moment M, inertia force of the rod $m_r(\frac{\partial^2 y}{\partial t^2})$ x, external force on the rod lateral surface $(q.\delta x)$, $(F_D.\delta x)$ viscous damping force, $F_L$ & $F_N$ drag forces per unit length in longitudinal and transverse direction, $F_I$ lateral force per unit length on the rod and is given by the change in momentum of lateral flow about the rod (12).

$$F_I = m_f \left(\frac{\partial}{\partial t} + V\frac{\partial}{\partial x}\right)^2 y \qquad \ldots \qquad (1)$$

where   $m_f$ = added virtual mass of the rod per unit length.

$$= \frac{\pi}{4} D^2 \rho C_M ,$$

here   $C_M$ = coefficient of added mass

   D = diameter of rod

   $\rho$ = density of fluid.

Rod material was postulated to obey stress-strain relation of Kelvin type, that is,

stress, $\sigma = \left( E\, e + \mu\, \dot{e} \right)$     . . .       (2)

where   E = Young's modulus of elasticity

     $\mu$ = Internal damping coefficient

     e = Strain and $\dot{e}$ = time derivative of strain.

Translatory and rotational equilibrium of the rod element leads to:

$$EI\, \frac{\partial^4 y}{\partial x^4} + \mu I \frac{\partial^5 y}{\partial x^4\, \partial t} + m_f \left( \frac{\partial}{\partial t} + V \frac{\partial}{\partial x} \right)^2 y + F_N + F_D$$

$$+ F_L\, \frac{\partial y}{\partial x} - T \frac{\partial^2 y}{\partial x^2} + m_r \frac{\partial^2 y}{\partial t^2} = q \qquad (3)$$

Drag forces for rough cylinder, as discussed by Taylor (33), are taken to be -

$$F_N = \frac{1}{2}\, \rho D V^2 \left( C_D\, \sin^2 \theta + C_f\, \sin \theta \right) \qquad (4)$$

$$F_L = \frac{1}{2}\, \rho D V^2\, C_f\, \cos \theta \qquad\qquad \ldots \qquad (5)$$

where $C_D$ and $C_f$ are drag coefficients due to pressure and shear forces. Angle $\theta$ is related to the normal and axial components of flow velocity by -

$$\theta = \sin^{-1} \left[ \frac{U}{V} \right] ,$$

where the normal component of velocity, $U = \left( \frac{\partial y}{\partial t} + V \frac{\partial y}{\partial x} \right)$

The longitudinal tension is the sum of the applied tension

(external) and the one arising from the fluid friction.
For a rod, supported at both ends, the initial tension
(axial) is taken as $T_O$ when $V = 0$ ; and as $V$ increases,
no further motion of the support is allowed. For a rod
with one end free, the initial tension is zero for $V = 0$,
but as $V$ increases, the free end is subjected to a tensile
force –

$$T (1 , t) = \frac{1}{2} \; C_T' \; m_f \; V^2 \qquad \ldots \qquad (6)$$

where $C_T'$ is the form drag coefficient at the free end.
Substitution of eqn. (5) into the equation of translatory
equilibrium and subsequent integration will give the
expression for the axial tension as –

$$T (x,t) = T_o + \frac{1}{2} \; C_T \; \frac{m_f \; V^2}{D} \; \left[ (1 - \tfrac{1}{2}\gamma) \, 1 - x \right]$$

$$+ \frac{1}{2} (1 - \gamma) \; C_T' \; m_f \; V^2 \qquad (7)$$

where $\gamma = 1$, if the downstream end is supported such that
the displacement is zero ; and $\gamma = 0$ if it is unsupported
or elastically supported.

The viscous damping force can be expressed as

$$F_D = C \quad \partial y / \partial t \qquad \ldots \qquad \ldots \qquad (8)$$

where $C$ is the effective viscous damping coefficient.
On substitution of eqns. (4), (5), (7) and (8) into eqn.
(3), will result in –

$$EI \frac{\partial^4 y}{\partial x^4} + \mu I \frac{\partial^5 y}{\partial t \partial x^4} + m_f V^2 \frac{\partial^2 y}{\partial x^2} - \gamma T_o \frac{\partial^2 y}{\partial x^2}$$

$$- \frac{1}{2} C_T \frac{m_f V^2}{D} \left[ (1 - \frac{1}{2}\gamma) \, 1 - x \right] \frac{\partial^2 y}{\partial x^2}$$

$$- \frac{1}{2} (1 - \gamma) C'_T m_f V^2 \frac{\partial^2 y}{\partial x^2} + 2 m_f V^2 \frac{\partial^2 y}{\partial x \partial t}$$

$$+ \frac{1}{2} (C_N + C_T) \frac{m_f V^2}{D} \frac{\partial y}{\partial x} + \frac{1}{2} C_N \frac{m_f V}{D} \frac{\partial y}{\partial t}$$

$$+ (m_r + m_f) \frac{\partial^2 y}{\partial t^2} = q (x, t) \tag{9}$$

The Boundary conditions of the system are :

for $x = 0$, $\quad k_1 \, y + EI \frac{\partial^3 y}{\partial x^3} = 0$ and $C_1 \frac{\partial y}{\partial x} - EI \frac{\partial^2 y}{\partial x^2} = 0$

$$\tag{10}$$

for $x = 1$, $\quad k_2 \, y - EI \frac{\partial^3 y}{\partial x^3} = 0$ and $C_2 \frac{\partial y}{\partial x} + EI \frac{\partial^2 y}{\partial x^2} = 0$

$$\tag{11}$$

where $C_1$, $C_2$ are the torsional stiffness and $k_1$, $k_2$ are displacement stiffness at two ends of the rod.

## APPENDIX-2

### Part (A)  Diffuser Dimensions:

Diffusers were used to connect the 6 inch pump line to the various size of test section.

| Test Section diameter (inches) | Length of diffuser (inches) | Semi Cone Angle (degrees) |
|---|---|---|
| 1.0 | 14.18 | 10 |
| 1.5 | 12.75 | 10 |
| 2.0 | 22.85 | 5 |
| 2.5 | 20.0 | 5 |

### Part (B)  V-Notch Characteristics:

Flow velocity in the test section was calculated from the head measurements over the V-notch, using the following relation :-

$$Q = C_d \cdot (H)^{2.481}$$

where  Q = Discharge in cubic feet/sec.

H = Head, over the crest, in feets.

$C_d$ = Coefficient of discharge.

For the V-notch used in the present study, value of the $C_d$ was 2.3974.

## APPENDIX-3

### Typical Values of R.M.S. Response

The horizontal and vertical component of the response are given below in the Tables 1 and 2.

### Table:1

Test-rod diameter    = 1/2 inch

Flow-tube diameter   = 2.5 inch

System amplifier     = 5000
gain

| Sl. No. | Velocity (ft./sec.) | Horizontal component (Milli-volts) r.m.s. | Vertical component (Milli-volts) r.m.s. |
|---------|---------------------|-------------------------------------------|------------------------------------------|
| 1. | 7.52 | 4.8 | 5.3 |
| 2. | 10.4 | 5.0 | 6.4 |
| 3. | 12.6 | 6.0 | 7.6 |
| 4. | 16.78 | 9.5 | 11.8 |
| 5. | 22.45 | 12.0 | 14.0 |
| 6. | 27.75 | 18.0 | 22.0 |
| 7. | 31.86 | 22.5 | 24.3 |
| 8. | 44.75 | 32.0 | 36.4 |

## Table:2

Test-rod diameter  = 1/2 inch

Flow-tube diameter = 1.0 inch

System amplifier  = 5000
gain

| Sl. No. | Velocity (ft./sec.) | Horizontal component (Milli-volts) r.m.s. | Vertical component (Milli-volts) r.m.s. |
|---------|---------------------|-------------------------------------------|-----------------------------------------|
| 1. | 6.18 | 6.0 | 7.1 |
| 2. | 9.2 | 8.5 | 11.6 |
| 3. | 15.34 | 18.0 | 22.8 |
| 4. | 20.7 | 32.0 | 36.5 |
| 5. | 27.6 | 56.0 | 63.0 |
| 6. | 36.5 | 61.5 | 78.0 |
| 7. | 42.1 | 89.5 | 115.0 |

These tables also indicate that the wall confinement
influences the horizontal signal in the similar way
as the vertical signal.

## ERRATA

| | written as | to be read as |
|---|---|---|
| Page 5 , line 11 | Stream | Steam |
| Page 7 , line 15 | These | The |
| Page 18, line 4 | 16 | <u>16</u> |
| Page 19, line 12 | Circuitory | Circuitry |
| Page 25, line 20 | hallow | hollow |
| Page 49, line 21 | 1.2 inch | 1.0 inch |